

HuPER: A Human-Inspired Framework for Phonetic Perception

Chenxu Guo ^{*1,2} Jiachen Lian ^{*2} Yisi Liu ² Baihe Huang ² Shriyaa Narayanan ² Cheol Jun Cho ²
Gopala Anumanchipalli ²

Abstract

We propose *HuPER*, a human-inspired framework that models phonetic perception as adaptive inference over acoustic-phonetics evidence and linguistic knowledge. With only 100 hours of training data, *HuPER* achieves state-of-the-art phonetic error rates on five English benchmarks and strong zero-shot transfer to 95 unseen languages. *HuPER* is also the first framework to enable adaptive, multi-path phonetic perception under diverse acoustic conditions. All training data, models, and code are open-sourced. Code and demo available at <https://github.com/HuPER29/HuPER>.

1. Introduction

Phonetic modeling is fundamental to speech perception. Early speech perception systems were expert systems (Davis et al., 1952; Erman et al., 1980; Lowerre, 1976; Baker, 1975; Rabiner, 2002) designed to emulate human perception, but constrained in scalability. Recent advances have demonstrated that large-scale word-based ASR (Radford et al., 2023; Zhang et al., 2023; Pratap et al., 2024; Omnilingual et al., 2025) can match or surpass human parity across domains. However, progress at the phonetic level remains limited, with little comparable gains despite similar scaling efforts. (Li et al., 2025). These observations motivate a human-centered rethinking of phonetic foundation models.

The human phonetic processor extracts acoustic-phonetic cues (Stevens, 2000; Mesgarani et al., 2014) and organizes them into hierarchical phonological representations for higher-level linguistic inference (Johnson, 2011). This process comprises a language-universal and an experience-dependent layer (Werker & Lalonde, 1988) encoding language-specific structure (Bhaya-Grossman et al., 2026). Both functions are dynamically shaped by bottom-up sensory evidence and top-down perceptual processes (Mes-

^{*}Equal contribution. ¹Zhejiang University, China ²University of California, Berkeley, USA. Correspondence to: Jiachen Lian <jiachenlian@berkeley.edu>.

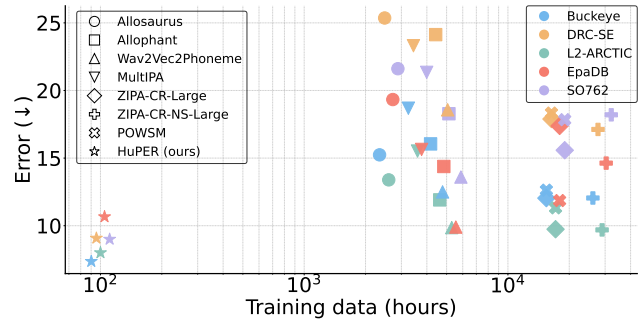


Figure 1. *HuPER* achieves highly data-efficient phonetic transcription on English variation benchmarks.

garani et al., 2014; Bhaya-Grossman et al., 2026).

Early self-supervised speech learning (S3L) models (Mohamed et al., 2022) can be viewed as analogous to infants' early exposure to continuous speech (Lavechin et al., 2023), during which broad acoustic-phonetic representations (Choi et al., 2024) are initially formed. However, subsequent fine-tuning (Xu et al., 2022; Chen et al., 2021) typically introduces lexical supervision *prematurely*. For instance, in fast speech, “last Sunday” is often realized as “las[] Sunday.” A developmentally plausible approach would supervise such surface forms first, allowing acoustic-phonetic representations to stabilize before higher-level abstraction. In contrast, most current phonetic models rely on G2P-derived canonical targets (Rudnicky, 1993; Mortensen et al., 2018; Black & Lenzo, 2001) (e.g., “last Sunday”), which encode phonological and grammatical regularities absent from the acoustic signal. This supervision mismatch prevents models from fully exploiting their acoustic-phonetic capacity and undermines subsequent phonological and lexical inference.

Beyond the premature introduction of lexical supervision, another open challenge is that human phonetic perception operates as a dynamic closed-loop system rather than a one-pass mapping from speech to phonemes (McClelland & Elman, 1986; Hickok & Poeppel, 2007; Norris et al., 2003). Most phoneme recognition models implicitly assume a unidirectional, feedforward processing pipeline. However, under ambiguous or degraded conditions, human listeners often engage top-down inference, using lexical or contextual expectations to constrain phonetic interpretation (War-

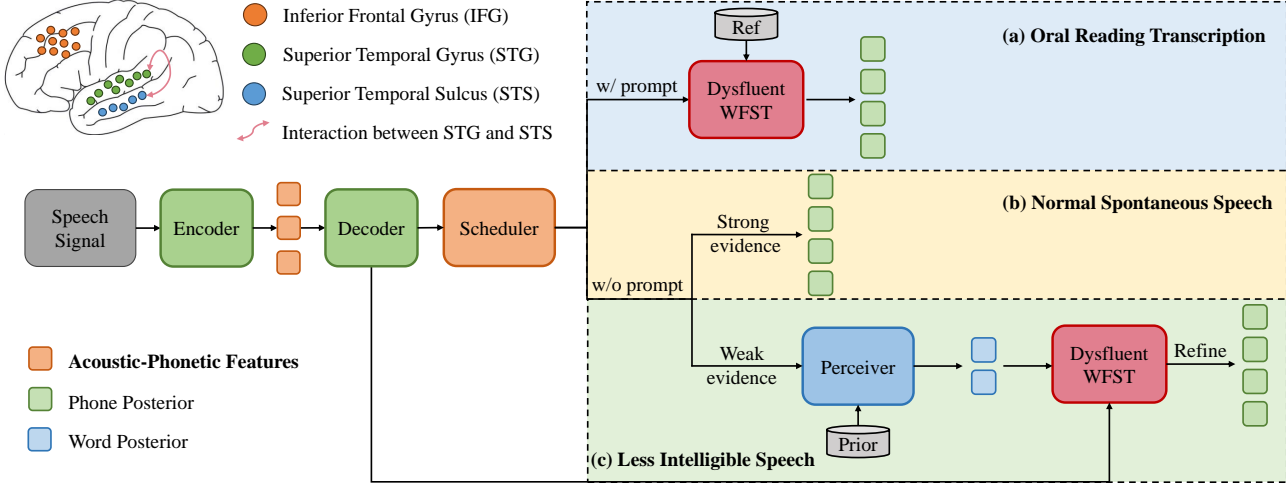


Figure 2. HuPER overview: evidence-controlled multi-path speech perception. Left: HuPER-Recognizer (Encoder/Decoder; mapped to STG) converts the speech signal into acoustic–phonetic features (orange) and phone posteriors (green). HuPER-Scheduler (mapped to IFG) monitors evidence strength and selects an inference route. Right: (a) *Oral reading transcription*: with an external prompt/reference, a Dysfluent WFST applies explicit top-down constraints to produce the transcript. (b) *Normal spontaneous speech*: when evidence is strong, the system trusts bottom-up phone evidence and outputs directly. (c) *Less intelligible speech*: when evidence is weak, HuPER-Perceiver combines phone evidence with a lexical prior to form word hypotheses (blue), which are then refined by the Dysfluent WFST (Guo et al., 2025).

ren, 1970; Ganong, 1980; Samuel, 2001), which in turn refines higher-level representations (McClelland & Elman, 1986; Norris et al., 2003). Notably, even when top-down information is available, listeners can deliberately rely on bottom-up processing when instructed or required by task demands (Cutler, 2012), indicating flexible cognitive control (Posner & Petersen, 1989; Norman & Shallice, 1986). Moreover, when reference text is available, as in performed or rehearsed speech, perception follows another pathway guided by explicit expectations (Lian et al., 2024). In contrast, most current AI systems implement a single feedforward route and lack mechanisms for modeling such multi-path, closed-loop dynamics.

Given these limitations, we propose **HuPER (A Human-Inspired Framework for Phonetic Perception)**, a human-centered framework that models phonetic perception as adaptive inference integrating acoustic evidence and linguistic knowledge. HuPER departs from conventional end-to-end pipelines by explicitly coordinating bottom-up cues and top-down expectations for robust, context-aware perception. Our main contributions are summarized as follows:

- (1) We present HuPER, the first unified and explicit computational framework for modeling human phonetic perception, which also provides a diagnostic perspective on existing phoneme recognition models.
- (2) HuPER achieves state-of-the-art phonetic accuracy with only 100 hours of training data, reaching an average PFER=8.82 on English benchmarks and demonstrating decent zero-shot multilingual transfer.

(3) We propose an adaptive multi-path inference mechanism for phonetic perception, enabling dynamic pathway selection and improved robustness under degraded and disordered speech conditions.

2. HuPER overview

We propose **HuPER (Human-Perceptual Phonetic Encoder)**, a modular speech perception framework that supports adaptive multi-path inference by integrating bottom-up acoustic–phonetic modeling with explicit top-down constraints, serving as an approximation to human cognitive speech perception systems (McClelland & Elman, 1986; Norris et al., 2003). As shown in Figure 2, HuPER consists of three functional modules and a central scheduler:

- (1) **HuPER-Recognizer** (STG-like, Bottom-Up Acoustic–Phonetic Perception, Sec. 3). It extracts language-general acoustic–phonetic evidence and outputs spoken phones, providing the foundational representation for downstream modules and determining the upper bound of universal phonetic perception. We further develop a self-training procedure for HuPER-Recognizer, which is theoretically grounded in our DRRC framework.
- (2) **HuPER-Perceiver** (STS-like, Phonetic–Lexical Integration, Sec. 4). It combines acoustic–phonetic representations with explicit lexical and phonotactic priors to generate phonetic-enhanced word hypotheses.
- (3) **Dysfluent WFST** (explicit top-down constraints; (Guo et al., 2025)). It provides a human-inspired, top-down constraint mechanism by representing dysfluencies and pronunciation variants in a WFST constraint graph, which can be

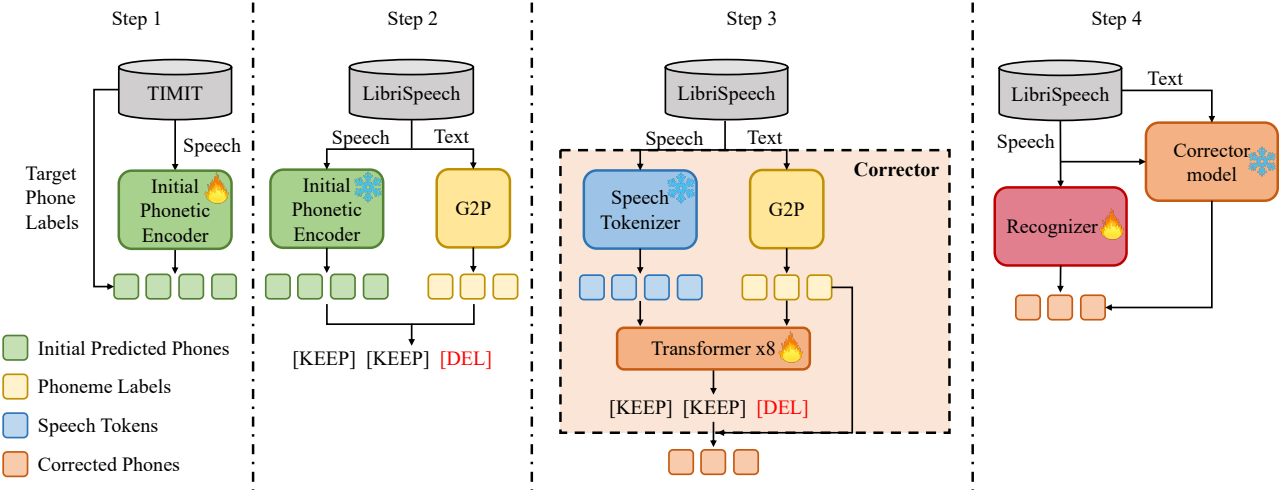


Figure 3. HuPER-Recognizer self-learning pipeline. The training procedure consists of four stages. (1) An initial phone recognizer is trained on a small human-annotated corpus (TIMIT) to produce acoustic phone predictions. (2) The recognizer is applied to a large transcript-only corpus (LibriSpeech) to generate teacher pseudo phones from speech, while a G2P system produces canonical phoneme sequences from text. (3) A Corrector model learns edit operations (keep, delete, substitute, insert) that transform canonical G2P phones into acoustically grounded phone proxies, using both speech tokens and G2P phones as input. (4) The recognizer is retrained on the large corpus using corrected pseudo phone labels, yielding a more robust and language-generalizable phone recognizer.

conditioned on external references or on hypotheses. **(4) HuPER-Scheduler** (IFG-like, Sec. 5). The scheduler selects inference pathways based on signal quality and task context. For clear speech, HuPER relies on bottom-up inference. Under degraded or ambiguous conditions, it integrates HuPER-Perceiver outputs with Dysfluent WFST constraints. In reference-guided scenarios (Lian et al., 2024), known intended text is incorporated through the constraint graph. We detail each part in the following sections.

3. HuPER-Recognizer

Task definition and outputs. The HuPER-Recognizer is a WavLM-Large model (Chen et al., 2021) fine-tuned for phone recognition. Given a speech signal X , it outputs phone posteriors and a decoded phone sequence \hat{Y}_θ . We treat \hat{Y}_θ as the *spoken phone* (i.e., what a human would perceive from the acoustics), and we aim to learn phone evidence that generalizes across languages.

To scale beyond scarce human phone labels, a common approach is self-training: generate pseudo phone labels on a large transcript-only set and retrain the recognizer on them (Lee, 2013; Xie et al., 2020). However, naive pseudo-label training can amplify systematic errors (confirmation bias) and can be statistically biased when the availability of true phone labels is not random.

We address these issues by introducing **doubly robust risk correction (DRRC)**. Concretely, we (i) construct proxy phone supervision on \mathcal{D}' via a phoneme→phone Corrector (Algorithm 1), and (ii) view the resulting training problem

as missing-label learning and analyze it through a DRRC objective (Sec. 3).

HuPER self-learning strategy. Figure 3 summarizes the recipe for constructing proxy phone supervision on a large transcript-only dataset. We use a small labeled set $\mathcal{D} = \{(X_i, Y_i)\}$ with human-verified phones and a transcript-only set $\mathcal{D}' = \{(X_j, T_j)\}$. For each $(X, T) \in \mathcal{D}'$, we compute a canonical phoneme sequence $Z = \text{G2P}(T)$, obtain a teacher phone hypothesis \bar{Y} from the current recognizer, and apply a Corrector to produce a corrected proxy phone sequence \hat{Y} . Algorithm 1 summarizes the iterative training procedure.

DRRC perspective. To formalize our analysis, we define the true population risk for a fixed HuPER-Recognizer parameter θ as

$$R(\theta) := \mathbb{E}[\ell_\theta(e(Y), X)], \quad (1)$$

where Y represents the latent true phone label (observed only on \mathcal{D}), and \hat{Y} denotes an always-observed proxy (derived from the teacher or the Corrector). Treating the canonical phoneme sequence $Z = \text{G2P}(T)$ as an auxiliary covariate, we cast self-training as a *missing data problem* (Robins et al., 1994; Bang & Robins, 2005) in which the observability of the true label Y is governed by Z via the true propensity function:

$$g^*(z, \hat{y}) := \mathbb{P}(A = 1 \mid Z = z, \hat{Y} = \hat{y}). \quad (2)$$

Practically, this formulation assumes that the transcript contains sufficient auxiliary information, distinct from the fea-

Algorithm 1 HuPER self-learning strategy

Input: human-labeled phone dataset $\mathcal{D} = \{(X_i, Y_i)\}$; transcript-only dataset $\mathcal{D}' = \{(X_j, T_j)\}$; G2P function $G2P(\cdot)$; Corrector $C(\cdot)$; number of rounds R

Output: HuPER-Recognizer $f^{(R)}$

Train initial recognizer $f^{(0)}$ on \mathcal{D} with CTC loss.

for $r = 0$ **to** $R - 1$ **do**

- Initialize pseudo-labeled set $\tilde{\mathcal{D}}^{(r)} = \emptyset$.
- for** each (X, T) **in** \mathcal{D}' **do**

 - $Z \leftarrow G2P(T)$ (canonical phoneme sequence)
 - $\bar{Y}^{(r)} \leftarrow f^{(r)}(X)$ (teacher phone prediction)
 - $\tilde{Y}^{(r)} \leftarrow C(X, Z; \bar{Y}^{(r)})$ (corrected pseudo phones; $\tilde{Y}^{(r)}$ optional)
 - $\tilde{\mathcal{D}}^{(r)} \leftarrow \tilde{\mathcal{D}}^{(r)} \cup \{(X, \tilde{Y}^{(r)})\}$

- end for**
- Train $f^{(r+1)}$ on $\tilde{\mathcal{D}}^{(r)}$ (optionally together with \mathcal{D}).

end for

return $f^{(R)}$

tures captured by the teacher model f_T , to distinguish the pseudo-label \hat{Y} from the true label Y (but not necessarily to fully recover the true label Y). We demonstrate that there exists a corrector such that the HuPER loss yields a *doubly robust* estimate of $R(\theta)$ on the self-training dataset. Specifically, the estimator is consistent if either (i) the propensity model for missing phone labels is correctly specified, or (ii) the proxy label \hat{Y} is (asymptotically) accurate.

Theorem 3.1 (Informal version of Theorem B.5). *For any measurable $g : \mathcal{Z} \times \{1, \dots, K\} \rightarrow (0, 1]$, define*

$$C_g(W) := e(\hat{Y}) + \frac{A}{g(Z, \hat{Y})} (e(Y) - e(\hat{Y})). \quad (3)$$

Let \hat{g} be a cross-fitted estimator clipped to $[\varepsilon, 1]$ and define

$$\hat{R}_n(\theta) := \frac{1}{n} \sum_{i=1}^n \ell_\theta(C_{\hat{g}}(W_i), X_i). \quad (4)$$

Then $\mathbb{E}[\ell_\theta(C_g(W), X)] = R(\theta)$ provided either **(G)**: $g = g^*$ or **(Y)**: $\hat{Y} = Y$. Furthermore, $\hat{R}_n(\theta) \rightarrow R(\theta)$ in probability provided either:

$$(\mathbf{G}): \mathbb{E}[|\hat{g}(Z, \hat{Y}) - g^*(Z, \hat{Y})|] \rightarrow 0, \text{ or } (\mathbf{Y}): \mathbb{P}(\hat{Y} \neq Y) \rightarrow 0. \quad (5)$$

This theorem shows that the corrected target $C_g(W)$ recovers the true risk $R(\theta)$ in expectation, and the empirical estimator is consistent when either the proxy labels are accurate (**Y**) or the propensity model is correct (**G**). Thus, DRRC is robust to misspecification of either component alone.

In summary, we scale HuPER-Recognizer with a phoneme→phone Corrector (Algorithm 1) and analyze the resulting self-learning objective through DRRC, which is

consistent under either accurate proxies or a correct propensity model. Next, HuPER-Perceiver converts the phone evidence into word transcripts using explicit lexical and LM constraints.

4. HuPER-Perceiver

HuPER-Perceiver converts HuPER-Recognizer’s *phone evidence* into word transcripts by composing it with explicit, auditable language constraints, following the classic HMM–GMM decoding recipe (acoustic model + lexicon + language model) but with a phone recognizer as the evidence source (Rabiner, 2002; Mohri et al., 2002). Given an utterance X and recognizer parameters θ , the output is a word sequence \hat{T} .

Acoustic evidence as a phone lattice. Rather than using only the 1-best phone sequence \hat{Y}_θ , we represent the recognizer output as a weighted phone acceptor (phone lattice) $\Pi_\theta(X)$. Each path y in $\Pi_\theta(X)$ corresponds to a candidate phone sequence, and is assigned a cost $C_\theta(y \mid X)$ derived from the negative log evidence (e.g., frame-level phone posteriors or arc weights). The decoded phone sequence \hat{Y}_θ is simply the best path in this lattice, while $\Pi_\theta(X)$ retains uncertainty needed for downstream constrained search.

Imposing lexical and linguistic constraints. To map phone hypotheses to words, we introduce a phone-to-word transducer L (lexicon) and a word-level acceptor G (language model). L restricts which phone sequences realize valid words, and G provides sequence-level linguistic preferences. Both L and G are modular constraints that can be swapped across domains without retraining the HuPER-Recognizer.

Search via WFST composition. Decoding is performed by composing the phone evidence with the constraints and extracting the shortest path in the unified search space:

$$\hat{T} = \text{Output}(\text{ShortestPath}(\Pi_\theta(X) \circ L \circ G)). \quad (6)$$

5. HuPER-Scheduler

The HuPER-Scheduler acts as the system’s *planner*, orchestrating the flow between bottom-up phone evidence and top-down linguistic expectations. By evaluating an *evidence distortion score* $s(X)$ computed from HuPER-Recognizer emissions, it decides whether to decode phones directly, or to activate a reference-constrained refinement path. In the guided path, we compile a *Dysfluent WFST* constraint $\mathcal{H}(\cdot)$ from a reference word sequence (external R or Perceiver 1-best hypothesis \hat{T}), and refine phone decoding by composing \mathcal{H} with the recognizer evidence (Guo et al., 2025; Mohri et al., 2002). Algorithm 2 summarizes the routing logic.

Algorithm 2 HuPER-Scheduler: distortion-controlled reference-constrained phone refinement

Input: utterance X ; phone evidence graph $\Pi_\theta(X)$; lexicon L ; LM G ; threshold τ ; optional external reference R

Output: final phone sequence \hat{Y}

Compute $s(X)$ using Equation 8.

if $s(X) \leq \tau$ **then**

$\hat{Y} \leftarrow \text{Output}(\text{ShortestPath}(\Pi_\theta(X)))$.

else

if R is available **then**

$U \leftarrow R$.

else

$\hat{T} \leftarrow \text{Output}(\text{ShortestPath}(\Pi_\theta(X) \circ L \circ G))$.

$U \leftarrow \hat{T}$.

end if

Compile Dysfluent WFST constraint $\mathcal{H} \leftarrow \mathcal{H}(U)$.

$\hat{Y} \leftarrow \text{Output}(\text{ShortestPath}(\Pi_\theta(X) \circ \mathcal{H}))$.

end if

return \hat{Y}

Quantifying Evidence Distortion. To assess signal reliability, the Scheduler monitors the Recognizer’s frame-level logits $\mathbf{z} \in \mathbb{R}^{T \times V}$ and posteriors $\mathbf{p}_t = \text{softmax}(\mathbf{z}_t)$. We quantify uncertainty through the posterior margin m_t and normalized entropy h_t :

$$m_t := p_{t,(1)} - p_{t,(2)}, \quad h_t := \frac{-\sum_{v=1}^V p_{t,v} \log p_{t,v}}{\log V}. \quad (7)$$

These are combined into a frame-level distortion proxy $d_t := \text{clip}(\frac{1}{2}(1 - m_t) + \frac{1}{2}h_t, 0, 1)$, and aggregated into an utterance-level score

$$s(X) := \frac{1}{T} \sum_{t=1}^T d_t, \quad (8)$$

which drives routing decisions.

Dysfluent WFST constraint $\mathcal{H}(\cdot)$. Given a reference word sequence U (either an external reference R or a hypothesis \hat{T}), the Dysfluent WFST compiles a phone-space constraint $\mathcal{H}(U)$, which encodes a bounded set of plausible *realized* phone sequences around the canonical pronunciation of U , while allowing dysfluent edits (insertions/deletions/substitutions) (Guo et al., 2025). This constraint is then combined with the HuPER-Recognizer phone evidence for constrained shortest-path inference.

6. Experimental setup

As described in Sec. 5, the HuPER-Scheduler supports three tasks: (1) **Task 1:** Speech-only transcription with strong acoustic evidence, corresponding to standard phoneme

recognition. (2) **Task 2:** Speech-only transcription under varying signal quality, where the scheduler adaptively selects between a purely bottom-up path (for strong evidence) and a combined bottom-up-top-down path (for weak evidence). (3) **Task 3:** Transcription with reference text provided, in which bottom-up and top-down perception are jointly performed. For **Task 1**, we conduct *phone recognition* experiments (Sec. 6.1). For **Tasks 2 and 3**, we conduct *multi-path speech perception* experiments (Sec. 6.2).

6.1. Phone recognition

Setup. We use WavLM-Large as the backbone and fine-tune it with a CTC (Graves et al., 2006) objective for phone recognition. Training follows our self-learning recipe. We first train an initial HuPER-Recognizer on TIMIT (Garofolo et al., 1993). We then apply this initial model to LibriSpeech (Panayotov et al., 2015) to obtain teacher pseudo phone labels, and train a correction model (Sec. 3) that refines the canonical G2P (Mortensen et al., 2018; Black & Lenzo, 2001; Zhu et al., 2022) phone sequence using acoustic evidence. The Corrector is trained for 49 epochs (about 40 minutes) on $2 \times$ A6000 GPUs. Audio is tokenized with HuBERT (Hsu et al., 2021) units. We use dropout 0.2, AdamW (Loshchilov & Hutter, 2017) with $\beta = (0.9, 0.999)$, and learning rate 2×10^{-4} . Finally, we train HuPER-Recognizer on the corrected pseudo labels for 100 epochs on $8 \times$ A6000 GPUs (batch size 12, learning rate 3×10^{-5}). We freeze the WavLM transformer for the first 24k updates and train only the linear CTC head, then unfreeze all WavLM layers for full fine-tuning. The final CTC training loss is 0.036.

Evaluation metric: PFER. We report **Phonetic Feature Error Rate (PFER)**, a PanPhon-based articulatory-feature edit distance widely used in multilingual phone recognition (Mortensen et al., 2016). PFER computes a minimum-cost edit distance between hypothesis and reference phone sequences, where substitutions are weighted by distinctive-feature differences (thus giving partial credit to phonetically similar phones), and is normalized by the reference length. Formal definition and costs are provided in Appx. D.

Baselines. We compare against widely used open-source universal phone recognizers (Table 9): **Allosaurus** (Li et al., 2020), **Allophant** (Glocke et al., 2023), **W2V2-eSpeak** (Xu et al., 2022; Baevski et al., 2020; Conneau et al., 2021), **Multipa** (Chen et al., 2024), **Zipa** (Zhu et al., 2025), and **POWSM** (Li et al., 2025).

Evaluation datasets. We evaluate only on corpora with *human-annotated* or *human-verified* phone labels, so the error rates are grounded in human perception rather than automatic alignments. Following the categorization used

in the attached paper, we group test sets into *English variation* and *unseen-language transfer*. Dataset statistics and evaluation splits are summarized in Table 7.

English variation. We evaluate on Buckeye (Pitt et al., 2005), which contains spontaneous conversational English. To probe dialectal variation, we additionally test on DRC-SE (DoReCo South-England), a dialect subset from DoReCo (Paschen et al., 2020). To measure robustness to non-native pronunciations, we evaluate on L2-ARCTIC (Zhao et al., 2018), EpaDB (Vidal et al., 2019), and SpeechOcean762 (Zhang et al., 2021), which contain L2 English speech with verified phone-level annotations. For L2-ARCTIC, we use the manually annotated *perceived* transcriptions rather than dictionary/G2P pronunciations, so the reference reflects what speakers actually produced.

Unseen languages (zero-shot). We further test multilingual transfer on VoxAngeles (Chodroff et al., 2024), a post-processed version of the UCLA Phonetics Lab Archive with human-verified transcriptions spanning 95 languages. This setting evaluates zero-shot generalization to languages and phone inventories never seen during training.

6.2. Multi-path speech perception

Dataset. For both **Task-2** and **Task-3**, we evaluate on a primary progressive aphasia (PPA) reading dataset (Gorno-Tempini et al., 2011) (nfvPPA, 35 speakers). We manually annotated *spoken* phone sequences (1h1m12s total). Each utterance provides audio X , a passage text R (available but optionally hidden), and a human phone reference Y .

Experimental Configuration. For **Task-3**, we follow the Dysfluent-WFST pipeline (Guo et al., 2025), replacing the original phonetic encoder with our HuPER-Recognizer. For **Task-2** with dynamic planning, we first compute a distortion score $s(X)$ from HuPER-Recognizer posteriors (Sec. 5) to characterize recognition difficulty. We then analyze whether $s(X)$ correlates with recognition performance and whether hypothesis-guided constrained decoding provides greater benefits than bottom-up 1-best decoding under high distortion. For both tasks, we treat the switching threshold τ as an externally specified hyperparameter and report results across a sweep of τ . The distortion-based configuration for **Task-2** is presented as follows:

Distortion Computation (Task-2). For each utterance, we compute an utterance-level distortion score $s(X)$ by aggregating the frame-level proxy $\{d_t\}_{t=1}^T$ defined in Sec. 5. We compare two phonetic encoders (HuPER and Wav2Vec2Phoneme (Xu et al., 2022)) under three decoding modes: (i) **1-best**: CTC decoding from phone evidence $\Pi(X)$; (ii) **refine**: constrained decoding with a hypothesis-conditioned WFST $\mathcal{H}(\hat{T}(X))$ (Guo et al., 2025) built from

Perceiver hypotheses. We report Spearman’s rank correlation coefficient ρ between $s(X)$ and PFER across PPA utterances to validate $s(X)$ as an uncertainty proxy (Fig. 6a).

Dynamic Switching Analysis (Task-2). To quantify when constrained inference is beneficial under dynamic planning, we define a distortion-threshold switch between HuPER 1-best and HuPER refine decoding:

$$\hat{Y}_\tau(X) = \begin{cases} \hat{Y}_{1\text{best}}(X), & s(X) \leq \tau, \\ \hat{Y}_{\text{refine}}(X), & s(X) > \tau, \end{cases} \quad (9)$$

We report the average PFER as a function of τ to identify distortion regimes in which constrained decoding yields the largest gains.

7. Result

7.1. Task-1: English phone recognition

HuPER-Recognizer achieves the best average PFER with orders-of-magnitude less supervision and a more compact label space, demonstrating the effectiveness and transferability of our DRRC-based acoustic-phonetic learning. Table 1 reports PFER on five corpora with human-annotated (or human-verified) phone labels. HuPER-Recognizer achieves the **best average** PFER (8.82) while using only 100 hours of English training data, whereas all compared baselines rely on orders-of-magnitude more supervision. This result highlights that our DRRC recipe (Sec. 3) can turn a small amount of human phone annotation into strong, transferable acoustic-phonetic evidence. We note that HuPER uses a compact phone inventory with only 42 symbols, which is smaller than the vocabularies used by several baselines. A smaller inventory reduces representational resolution and can make certain fine-grained contrasts unexpressible, which may disadvantage HuPER under PFER (a feature-sensitive edit distance). Therefore, the average-best performance is achieved despite a conservative label space.

7.2. Task-1: Zero-shot multilingual transfer

HuPER-Recognizer matches strong multilingual baselines in strict zero-shot cross-lingual transfer, despite being trained only on English. We evaluate cross-lingual generalization on VoxAngeles (95 languages) in a strict zero-shot setting. Trained only on English, HuPER-Recognizer achieves a macro-average PFER of 0.19. In contrast, a public English-only phoneme model Wav2Vec2-en, fine-tuned on G2P-generated phoneme labels from LJSpeech, yields a much higher PFER of 0.35. Figure 4 reports per-language results: HuPER improves over Wav2Vec2-en on the majority of languages, indicating robust transfer to unseen phone inventories. Moreover, among the multilingual baselines we evaluate, the best system (W2V2-eSpeak)

Table 1. PFER (↓) on human-annotated / human-verified phone datasets. All baseline numbers are reproduced using released checkpoints under a unified evaluation pipeline. Train (h) denotes the amount of training data reported/used by each model. DRC-SE = DoReCo South-England; SO762 = SpeechOcean762. *Allosaurus reports training scale in utterance counts; we convert to hours assuming an average utterance duration of 4 seconds.

Model	Train (h)	Buckeye	DRC-SE	L2-ARCTIC	EpaDB	SO762	Avg.
Allosaurus (Li et al., 2020)	2,600*	44.03	25.36	13.03	12.82	16.73	22.72
Allophant (Glocker et al., 2023)	4,628	35.04	24.13	11.91	14.03	18.11	20.66
W2V2-eSpeak (Xu et al., 2022)	5,300	27.50	18.57	8.77	9.59	14.62	15.83
MultiIPA (Chen et al., 2024)	3,600	18.69	23.31	15.52	15.64	21.34	18.28
ZIPA-CR-Large (Zhu et al., 2025)	17,132	31.24	17.89	9.74	11.75	15.58	17.24
ZIPA-CR-NS-Large (Zhu et al., 2025)	28,983	31.05	17.12	8.54	11.63	18.20	17.31
POWSM (Li et al., 2025)	17,132	31.63	18.33	11.32	11.86	17.84	18.68
HuPER-Recognizer (ours)	100	7.36	9.08	8.00	10.66	9.00	8.82

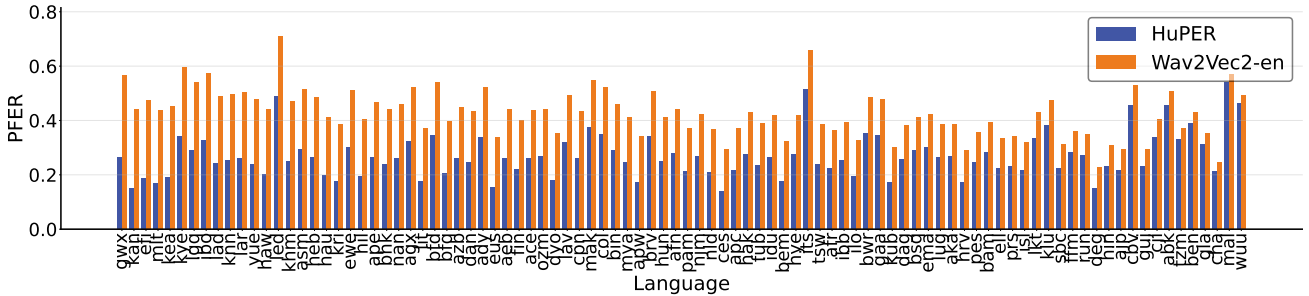


Figure 4. Zero-shot multilingual phone recognition on VoxAngeles (95 languages). Per-language phone error rate (PFER, ↓) for HuPER-Recognizer (trained only on English) and an English-only public phoneme model Wav2Vec2-en (fine-tuned on G2P-generated phoneme labels from LJSpeech). HuPER improves on the majority of languages and reduces the macro-average PFER from 0.35 to 0.19.

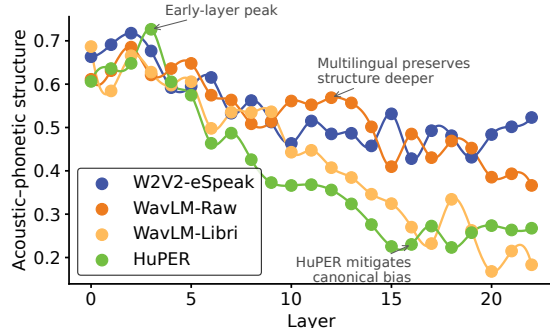


Figure 5. Centroid RSA to acoustic–phonetic geometry. Spearman correlation between pairwise phone-centroid cosine distances and PanPhon distinctive-feature distances across layers. Higher values indicate stronger acoustic–phonetic organization.

reaches an average PFER of 0.19, which HuPER matches despite being trained only on English. Full per-language results are provided in Table 8.

7.3. Flexible speech perception (Task2, Task3)

Task-3: HuPER-Recognizer consistently outperforms existing phonetic encoders on disordered speech, indicating more robust acoustic–phonetic representations.

With reference text, constrained decoding further improves robustness, and HuPER + reference achieves the best overall PFER on nfvPPA (Table 2), outperforming the Dysfluent-WFST baseline.

Task-2: HuPER achieves substantial gains under weak acoustic evidence through distortion-guided activation of top-down constraints. On nfvPPA, the distortion score correlates positively with HuPER 1-best PFER (Figure 6a), validating it as an uncertainty proxy. While HuPER 1-best already improves over Wav2Vec2, distortion-controlled switching yields the main gains, substantially reducing overall PFER (Table 2). Threshold analysis and distortion-bin breakdown (Figures 6b, 6c) show that improvements concentrate in high-distortion segments, where constrained decoding is most effective. Failure cases are discussed in Appendix E.

8. Understanding HuPER-Recognizer Gains

8.1. Embedding analysis: acoustic–phonetic geometry

HuPER maintains stronger alignment to distinctive-feature geometry in mid/late layers than an English G2P-supervised baseline. We measure layer-wise centroid RSA between phone representations and PanPhon distinctive-feature distances (Mortensen et al., 2016) on

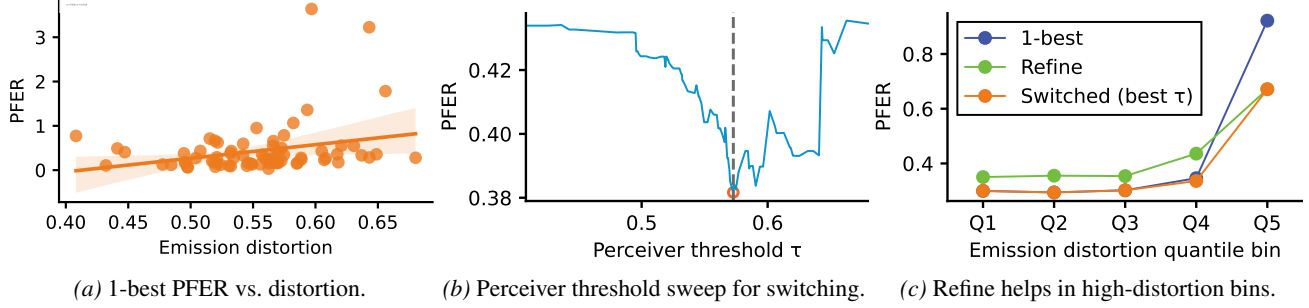


Figure 6. Distortion as a control signal for refinement on PPA. (a) Using HuPER 1-best throughout, emission distortion is positively correlated with PFER, indicating it tracks weak-evidence difficulty. (b) Sweeping the switching threshold τ reveals an optimal region for triggering refinement: we output 1-best when $s(X) \leq \tau$, and otherwise invoke the perceiver to decode words from phone evidence and refine the phone sequence. (c) Stratifying utterances by distortion explains why switching helps: refinement yields the largest gains in high-distortion regimes, while low-distortion cases are best handled by direct decoding.

Table 2. Weak-evidence speech perception on nfvPPA. Overall PFER for different decoding modes; HuPER-switched applies refinement only when $s(X) > \tau^*$ (refine rate shown).

Method	Overall PFER ↓	Refine rate
Wav2vec2 1-best	0.46	–
HuPER-recognizer 1-best	0.44	–
HuPER switched (τ^*)	0.38	31.1%
Dysfluent WFST	0.35	100%
HuPER + reference	0.32	100%

TIMIT. Figure 5 shows that all models peak in early layers (around layer 2–4), but **HuPER remains more aligned than WavLM-Libri deeper in the network**, suggesting DRRC-style acoustic correction helps preserve realized-phone structure beyond shallow acoustic features. Full RSA setup is in Appendix F.1, and additional acoustic/articulatory reference analyses are in Appendix C.

8.2. Emission analysis: canonical restoration

HuPER’s emissions consistently favor the realized sequence on the same acoustics, indicating less emission-level canonical “auto-correction” than an XLSR baseline. We evaluate controlled contrasts in three settings where canonical restoration is tempting: **glottalization**, **flaps**, and **stop reductions in clusters**. For each waveform, we compare CTC evidence for a canonical G2P sequence versus a manually verified realized sequence using a length-normalized preference score. Figure 7 shows that the XLSR baseline is more often canonical-restoring (especially for glottalization and cluster reductions), while **HuPER remains more acoustic-faithful**. This matches our design goal: bottom-up emissions should track available cues, and any canonical restoration should be applied explicitly by higher-level constraints when needed. Diagnostic-set construction, the exact score definition, and the full text/label

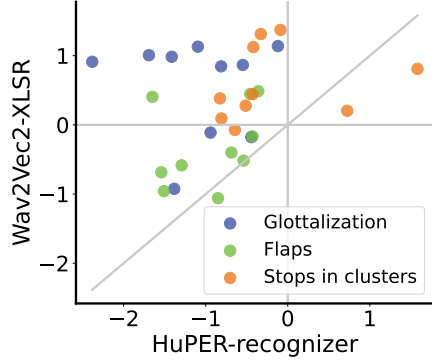


Figure 7. Emission-level canonical-restoration diagnostic. Scatter of canonical-vs-realized preference scores on identical utterances: HuPER (x-axis) vs. XLSR (y-axis), colored by category. Points above the diagonal ($y = x$) indicate stronger canonical restoration by the baseline.

pairs are provided in Appendix F.2.

9. Conclusion and Limitations

In this work, we view phonetic perception as an adaptive and controllable inference process and introduce HuPER as an initial step toward explicit, human-centered modeling. Our results highlight the value of combining phonetic representations, structured constraints, and dynamic control for robust and interpretable perception. However, the current system is still limited by the small amount of human-verified spoken-phone labels, relies on heuristic and rule-based routing, and models only a small subset of the inference pathways involved in real human perception. Addressing these limitations with larger annotated datasets, learned control policies, and more expressive perceptual models is an important direction for future work.

10. Acknowledgement

Thanks for support from UC Noyce Initiative, Society of Hellman Fellows, NIH/NIDCD, and the Schwab Innovation fund. We thank UCSF team for providing access to part of the clinical dataset used in this study.

Impact Statement

This work aims to advance speech and language technologies by improving the reliability and interpretability of phonetic representations. More accurate and acoustically grounded phonetic modeling can substantially benefit assistive applications in education, healthcare, and accessibility, where transcription errors and hallucinated outputs often undermine user trust and efficiency. By reducing such errors, HuPER has the potential to support more reliable screening, assessment, and communication tools for diverse populations. Beyond immediate applications, HuPER provides a scalable phonetic foundation that may facilitate the development of more expressive and flexible speech generation systems, including text-to-speech models based on acoustically meaningful tokens. More broadly, by framing speech perception as an adaptive and modular inference process, this work points toward future speech foundation systems that integrate perception, reasoning, and control, rather than isolated task-specific models.

References

AlKhamissi, B., De Sabbata, C. N., Tuckute, G., Chen, Z., Schrimpf, M., and Bosselut, A. Mixture of cognitive reasoners: Modular reasoning with brain-like specialization. *arXiv preprint arXiv:2506.13331*, 2025.

Angelaki, D., Benson, B., Benson, J., Birman, D., Bonacchi, N., Bougrova, K., Bruijns, S. A., Carandini, M., Catarino, J. A., et al. A brain-wide map of neural activity during complex behaviour. *Nature*, 645(8079):177–191, 2025.

Angelopoulos, A. N., Bates, S., Fannjiang, C., Jordan, M. I., and Zrnic, T. Prediction-powered inference. *Science*, 382 (6671):669–674, 2023.

Baevski, A., Zhou, Y., Mohamed, A., and Auli, M. wav2vec 2.0: A framework for self-supervised learning of speech representations. *Advances in neural information processing systems*, 33:12449–12460, 2020.

Baker, J. The dragon system—an overview. *IEEE Transactions on Acoustics, speech, and signal Processing*, 23(1): 24–29, 1975.

Bang, H. and Robins, J. M. Doubly robust estimation in missing data and causal inference models. *Biometrics*, 61 (4):962–973, 2005.

Bhaya-Grossman, I., Leonard, M. K., Zhang, Y., Gwilliams, L., Johnson, K., Lu, J., and Chang, E. F. Shared and language-specific phonological processing in the human temporal lobe. *Nature*, 649(8095):140–151, 2026.

Black, A. W. and Lenzo, K. A. Flite: a small fast run-time synthesis engine. In *SSW*, pp. 204, 2001.

Chen, S., Wang, C., Chen, Z., Wu, Y., Liu, S., Chen, Z., Li, J., Kanda, N., Yoshioka, T., Xiao, X., Wu, J., Zhou, L., Ren, S., Qian, Y., Qian, Y., Wu, J., Zeng, M., and Wei, F. Wavlm: Large-scale self-supervised pre-training for full stack speech processing. 2021.

Chen, Y.-W., Yu, Z., and Hirschberg, J. MultiPA: A Multi-task Speech Pronunciation Assessment Model for Open Response Scenarios. In *Interspeech 2024*, pp. 297–301, 2024. doi: 10.21437/Interspeech.2024-123.

Chodroff, E., Pazon, B., Baker, A., and Moran, S. Phonetic segmentation of the ucla phonetics lab archive. In Calzolari, N., Kan, M.-Y., Hoste, V., Lenci, A., Sakti, S., and Xue, N. (eds.), *LREC/COLING*, pp. 12724–12733. ELRA and ICCL, 2024. ISBN 978-2-493814-10-4.

Choi, K., Pasad, A., Nakamura, T., Fukayama, S., Livescu, K., and Watanabe, S. Self-Supervised Speech Representations are More Phonetic than Semantic. In *Interspeech 2024*, pp. 4578–4582, 2024. doi: 10.21437/Interspeech.2024-1157.

Conneau, A., Baevski, A., Collobert, R., Mohamed, A., and Auli, M. Unsupervised cross-lingual representation learning for speech recognition. In Hermansky, H., Cernocký, H., Burget, L., Lamel, L., Scharenborg, O., and Motíćek, P. (eds.), *Interspeech*, pp. 2426–2430. ISCA, 2021.

Cutler, A. *Native listening: Language experience and the recognition of spoken words*. Mit Press, 2012.

Davis, K. H., Biddulph, R., and Balashek, S. Automatic recognition of spoken digits. *The Journal of the Acoustical Society of America*, 24(6):637–642, 1952.

Erman, L. D., Hayes-Roth, F., Lesser, V. R., and Reddy, D. R. The hearsay-ii speech-understanding system: Integrating knowledge to resolve uncertainty. *ACM Computing Surveys (CSUR)*, 12(2):213–253, 1980.

Ganong, W. F. Phonetic categorization in auditory word perception. *Journal of Experimental Psychology: Human Perception and Performance*, 6(1):110–125, 1980.

Garofolo, J. S., of Standards, N. I., U.S., T., States, U., Agency., D. A. R. P., Science, I., Office, T., and Consortium., L. D. TIMIT : acoustic-phonetic continuous speech corpus., 1993.

Glocker, K., Herygers, A., and Georges, M. Allophant: Cross-lingual phoneme recognition with articulatory attributes. In *Interspeech 2023*, pp. 2258–2262, 2023. doi: 10.21437/Interspeech.2023-772.

Gorno-Tempini, M. L., Hillis, A. E., Weintraub, S., Kertesz, A., Mendez, M., Cappa, S. F., Ogar, J. M., Rohrer, J. D., Black, S., Boeve, B. F., et al. Classification of primary progressive aphasia and its variants. *Neurology*, 76(11): 1006–1014, 2011.

Graves, A., Fernández, S., Gomez, F., and Schmidhuber, J. Connectionist temporal classification: labelling unsegmented sequence data with recurrent neural networks. In *Proceedings of the 23rd international conference on Machine learning*, pp. 369–376, 2006.

Guo, C., Lian, J., Zhou, X., Zhang, J., Li, S., Ye, Z., Park, P., Das, A., Ezzes, Z., Vonk, J., Morin, B., Bogley, R., Wauters, L., Miller, Z., Gorno-Tempini, M. L., and Anumanchipalli, G. Dysfluent wfst: A framework for zero-shot speech dysfluency transcription and detection. In Scharenborg, O., Oertel, C., and Truong, K. (eds.), *INTERSPEECH*. ISCA, 2025.

Hickok, G. and Poeppel, D. The cortical organization of speech processing. *Nature reviews neuroscience*, 8(5): 393–402, 2007.

Hinton, G., Deng, L., Yu, D., Dahl, G. E., Mohamed, A.-r., Jaitly, N., Senior, A., Vanhoucke, V., Nguyen, P., Sainath, T. N., et al. Deep neural networks for acoustic modeling in speech recognition: The shared views of four research groups. *IEEE Signal processing magazine*, 29(6):82–97, 2012.

Hsu, W.-N., Bolte, B., Tsai, Y.-H. H., Lakhota, K., Salakhutdinov, R., and Mohamed, A. Hubert: Self-supervised speech representation learning by masked prediction of hidden units. *IEEE/ACM Transactions on Audio, Speech, and Language Processing*, 29:3451–3460, 2021. doi: 10.1109/TASLP.2021.3122291.

Huang, R., Li, M., Yang, D., Shi, J., Chang, X., Ye, Z., Wu, Y., Hong, Z., Huang, J., Liu, J., et al. Audiogpt: Understanding and generating speech, music, sound, and talking head. In *Proceedings of the AAAI Conference on Artificial Intelligence*, volume 38, pp. 23802–23804, 2024.

Johnson, K. *Acoustic and auditory phonetics*. John Wiley & Sons, 2011.

Kang, J. D. and Schafer, J. L. Demystifying double robustness: A comparison of alternative strategies for estimating a population mean from incomplete data. 2007.

Lavechin, M., Sy, Y., Titeux, H., Blandón, M. A. C., Räsänen, O., Bredin, H., Dupoux, E., and Cristia, A. Babyslm: language-acquisition-friendly benchmark of self-supervised spoken language models. In *Interspeech 2023*, pp. 4588–4592, 2023. doi: 10.21437/Interspeech.2023-978.

Lee, D.-H. Pseudo-label: The simple and efficient semi-supervised learning method for deep neural networks. In *ICML Workshop on Challenges in Representation Learning*, 2013.

Li, C.-J., Chang, K., Bharadwaj, S., Yeo, E., Choi, K., Zhu, J., Mortensen, D., and Watanabe, S. Powsm: A phonetic open whisper-style speech foundation model. *arXiv preprint arXiv:2510.24992*, 2025.

Li, X., Dalmia, S., Li, J., Lee, M., Littell, P., Yao, J., Anastopoulos, A., Mortensen, D. R., Neubig, G., Black, A. W., and Florian, M. Universal phone recognition with a multilingual allophone system. In *ICASSP 2020-2020 IEEE International Conference on Acoustics, Speech and Signal Processing (ICASSP)*, pp. 8249–8253. IEEE, 2020.

Lian, J., Zhou, X., Ezzes, Z., Vonk, J., Morin, B., Baquirin, D. P., Miller, Z., Gorno Tempini, M. L., and Anumanchipalli, G. Ssdm: Scalable speech dysfluency modeling. *Advances in neural information processing systems*, 37:101818–101855, 2024.

Liao, S.-H. Expert system methodologies and applications—a decade review from 1995 to 2004. *Expert systems with applications*, 28(1):93–103, 2005.

Liu, X., Zhu, Z., Liu, H., Yuan, Y., Huang, Q., Cui, M., Liang, J., Cao, Y., Kong, Q., Plumley, M. D., et al. Wavjourney: Compositional audio creation with large language models. *IEEE Transactions on Audio, Speech and Language Processing*, 2025.

Loshchilov, I. and Hutter, F. Decoupled weight decay regularization. *arXiv preprint arXiv:1711.05101*, 2017.

Lowerre, B. T. *The harpy speech recognition system*. Carnegie Mellon University, 1976.

Mark, G. and Steve, Y. The application of hidden markov models in speech recognition. *Foundations and Trends® in Signal Processing*, 1(3):195–304, 2024.

McClelland, J. L. and Elman, J. L. The trace model of speech perception. *Cognitive psychology*, 18(1):1–86, 1986.

Mesgarani, N., Cheung, C., Johnson, K., and Chang, E. F. Phonetic feature encoding in human superior temporal gyrus. *Science*, 343(6174):1006–1010, 2014.

Mohamed, A., Lee, H.-y., Borgholt, L., Havtorn, J. D., Edin, J., Igel, C., Kirchhoff, K., Li, S.-W., Livescu, K., Maaløe, L., et al. Self-supervised speech representation learning: A review. *IEEE Journal of Selected Topics in Signal Processing*, 16(6):1179–1210, 2022.

Mohri, M., Pereira, F., and Riley, M. Weighted finite-state transducers in speech recognition. *Computer Speech & Language*, 16(1):69–88, 2002.

Mortensen, D. R., Littell, P., Bharadwaj, A., Goyal, K., Dyer, C., and Levin, L. Panphon: A resource for mapping ipa segments to articulatory feature vectors. In *Proceedings of COLING 2016, the 26th International Conference on Computational Linguistics: Technical Papers*, pp. 3475–3484, 2016.

Mortensen, D. R., Dalmia, S., and Littell, P. Epitran: Precision g2p for many languages. In *Proceedings of the Eleventh International Conference on Language Resources and Evaluation (LREC 2018)*, 2018.

Norman, D. A. and Shallice, T. Attention to action: Willed and automatic control of behavior. In *Consciousness and self-regulation: Advances in research and theory volume 4*, pp. 1–18. Springer, 1986.

Norris, D., McQueen, J. M., and Cutler, A. Perceptual learning in speech. *Cognitive Psychology*, 47(2):204–238, 2003. doi: 10.1016/S0010-0285(03)00006-9.

Omnilingual, A., Keren, G., Kozhevnikov, A., Meng, Y., Ropers, C., Setzler, M., Wang, S., Adebara, I., Auli, M., Balioglu, C., et al. Omnilingual asr: Open-source multi-lingual speech recognition for 1600+ languages. *arXiv preprint arXiv:2511.09690*, 2025.

Panayotov, V., Chen, G., Povey, D., and Khudanpur, S. Librispeech: an asr corpus based on public domain audio books. In *Acoustics, Speech and Signal Processing (ICASSP), 2015 IEEE International Conference on*, pp. 5206–5210. IEEE, 2015.

Paschen, L. et al. Building a time-aligned cross-linguistic reference corpus from language documentation data (doreco). In *Proc. LREC*, 2020.

Pitt, M. A., Johnson, K., Hume, E., Kiesling, S., and Raymond, W. The buckeye corpus of conversational speech: Labeling conventions and a test of transcriber reliability. *Speech Communication*, 45(1):89–95, 2005.

Posner, M. I. and Petersen, S. E. The attention system of the human brain. 1989.

Pratap, V., Tjandra, A., Shi, B., Tomasello, P., Babu, A., Kundu, S., Elkahky, A., Ni, Z., Vyas, A., Fazel-Zarandi, M., et al. Scaling speech technology to 1,000+ languages. *Journal of Machine Learning Research*, 25(97):1–52, 2024.

Rabiner, L. R. A tutorial on hidden markov models and selected applications in speech recognition. *Proceedings of the IEEE*, 77(2):257–286, 2002.

Radford, A., Kim, J. W., Xu, T., Brockman, G., McLeavey, C., and Sutskever, I. Robust speech recognition via large-scale weak supervision. In *International conference on machine learning*, pp. 28492–28518. PMLR, 2023.

Robins, J. M., Rotnitzky, A., and Zhao, L. P. Estimation of regression coefficients when some regressors are not always observed. *Journal of the American statistical Association*, 89(427):846–866, 1994.

Rudnicky, A. The cmu pronouncing dictionary, 1993. Accessed October 2, 2025.

Samuel, A. G. Knowing a word affects the fundamental perception of the sounds within it. *Psychological Science*, 12(4):348–351, 2001.

Stevens, K. N. *Acoustic phonetics*, volume 30. MIT press, 2000.

Vidal, J., Ferrer, L., and Brambilla, L. A database for development of pronunciation assessment systems for english learners. In *Proc. Interspeech*, 2019.

Wager, S. and Athey, S. Estimation and inference of heterogeneous treatment effects using random forests. *Journal of the American Statistical Association*, 113(523):1228–1242, 2018.

Warren, R. M. Perceptual restoration of missing speech sounds. *Science*, 167(3917):392–393, 1970. doi: 10.1126/science.167.3917.392.

Werker, J. F. and Lalonde, C. E. Cross-language speech perception: Initial capabilities and developmental change. *Developmental psychology*, 24(5):672, 1988.

Xie, Q., Luong, M.-T., Hovy, E., and Le, Q. V. Self-training with noisy student improves imagenet classification. In *Proceedings of the IEEE/CVF Conference on Computer Vision and Pattern Recognition (CVPR)*, 2020.

Xu, Q., Baevski, A., and Auli, M. Simple and effective zero-shot cross-lingual phoneme recognition. In Ko, H. and Hansen, J. H. L. (eds.), *INTERSPEECH*, pp. 2113–2117. ISCA, 2022.

Zhang, J., Zhang, Z., Wang, Y., Yan, Z., Song, Q., Huang, Y., Li, K., Povey, D., and Wang, Y. Speechocean762: An open-source non-native english speech corpus for pronunciation assessment. In *Proc. Interspeech*, 2021.

Zhang, Y., Han, W., Qin, J., Wang, Y., Bapna, A., Chen, Z., Chen, N., Li, B., Axelrod, V., Wang, G., et al. Google usm: Scaling automatic speech recognition beyond 100 languages. *arXiv preprint arXiv:2303.01037*, 2023.

Zhao, G., Sonsaat, S., Silpachai, A., Lucic, I., Chukharev-Hudilainen, E., Levis, J., and Gutierrez-Osuna, R. L2-arctic: A non-native english speech corpus. In *Proc. Interspeech*, 2018.

Zhou, X., Lian, J., Hong, H., Yang, X., and Anumanchipalli, G. Speech world model: Causal state-action planning with explicit reasoning for speech. *International Conference on Learning Representations*, 2026.

Zhu, J., Zhang, C., and Jurgens, D. Byt5 model for massively multilingual grapheme-to-phoneme conversion. In Ko, H. and Hansen, J. H. L. (eds.), *INTERSPEECH*, pp. 446–450. ISCA, 2022.

Zhu, J., Samir, F., Chodroff, E., and Mortensen, D. R. Zipa: A family of efficient models for multilingual phone recognition. In Che, W., Nabende, J., Shutova, E., and Pilehvar, M. T. (eds.), *ACL (1)*, pp. 19568–19585. Association for Computational Linguistics, 2025. ISBN 979-8-89176-251-0.

A. Related Work

Phonetic recognition models Traditional phonetic models have been closely co-developed with ASR paradigms and are primarily data-driven, relying on lexicon-derived targets and large-scale supervision, evolving from HMM–GMM (Rabiner, 2002; Mark & Steve, 2024) systems to hybrid HMM–DNN (Hinton et al., 2012) and end-to-end architectures (Graves et al., 2006). Such systems (Li et al., 2020; Glocker et al., 2023) assign canonical phonemes rather than realized phones, and progress in phone recognition has therefore depended heavily on costly manual annotations. In parallel, linguistically driven approaches incorporate phonological and articulatory priors (Mortensen et al., 2016), such as distinctive features and allophonic modeling, to improve generalization and cross-lingual transfer, but rely on curated linguistic resources and handcrafted representations, limiting their scalability. From a cognitive perspective, phoneme perception itself is a multi-path, closed-loop process that integrates bottom-up acoustic evidence with top-down linguistic and contextual expectations (McClelland & Elman, 1986; Norris et al., 2003). To date, these three paradigms remain largely disconnected.

Explicit modeling of human-inspired speech perception Early expert systems (Liao, 2005) attempted to emulate human cognition through rigid pipelines, which were later shown not to be faithful proxies (Angelaki et al., 2025), as cognition emerges from dynamic interactions among functional modules. While cognitive language models, such as (AlKhamissi et al., 2025), introduce brain-inspired modular specialization, these designs remain domain-specific and are not tailored to speech perception. In the context of speech modeling, audio agents (Huang et al., 2024; Liu et al., 2025) focus on high-level task orchestration and act mainly as wrappers around existing models, without explicitly modeling perceptual mechanisms. Speech world models (Zhou et al., 2026) represent early attempts to modularize speech perception, but operate primarily at the prompt level rather than directly decomposing perceptual representations.

B. Doubly Robust Consistency of HuPER Corrector

B.1. Setup and notation

Fix $K \geq 2$. Let $W = (X, Z, Y, \hat{Y}, A)$ be a generic draw, where: (i) X are features used by a predictive model $p_\theta(\cdot | X)$, (ii) Z are covariates governing label missingness, (iii) $Y \in \{1, \dots, K\}$ is the true class label, (iv) $\hat{Y} \in \{1, \dots, K\}$ is an always-observed proxy label, (v) $A \in \{0, 1\}$ indicates whether Y is observed (so AY is observed, but Y may be missing when $A = 0$). Let $e(k) \in \mathbb{R}^K$ denote the one-hot vector with a 1 in coordinate k . Write $e(Y)$ and $e(\hat{Y})$ for the corresponding (random) one-hot vectors of Y and \hat{Y} . Define the multiclass log-loss for any label vector $q \in \mathbb{R}^K$ by

$$\ell_\theta(q, x) := - \sum_{k=1}^K q_k \log p_\theta(k | x).$$

In particular, $\ell_\theta(e(Y), X) = -\log p_\theta(Y | X)$. The target population risk is

$$R(\theta) := \mathbb{E}[\ell_\theta(e(Y), X)].$$

Define the score vector $s_\theta(X) \in \mathbb{R}^K$ by $s_{\theta,k}(X) := -\log p_\theta(k | X)$, so that

$$\ell_\theta(q, X) = q^\top s_\theta(X).$$

Missingness model and nuisance functions. Define the true propensity (missingness) function

$$g^*(z, \hat{y}) := \mathbb{P}(A = 1 | Z = z, \hat{Y} = \hat{y}).$$

Define also the conditional class distribution given the always-observed variables $V := (X, Z, \hat{Y})$:

$$f^*(x, z, \hat{y}) := \mathbb{E}[e(Y) | X = x, Z = z, \hat{Y} = \hat{y}] \in \Delta_K,$$

where $\Delta_K := \{q \in \mathbb{R}^K : q_k \geq 0, \sum_{k=1}^K q_k = 1\}$.

Proxy-baseline AIPW corrector. For any measurable $g : \mathcal{Z} \times \{1, \dots, K\} \rightarrow (0, 1]$, define

$$C_g(W) := e(\hat{Y}) + \frac{A}{g(Z, \hat{Y})} (e(Y) - e(\hat{Y})).$$

Note that $C_g(W)$ need not lie in Δ_K (it can have negative entries when $A = 1$ and $g(Z, \hat{Y}) < 1$), but $\ell_\theta(\cdot, X)$ is linear in its first argument, so $\ell_\theta(C_g(W), X)$ is well-defined.

Cross-fitted risk estimator. Let W_1, \dots, W_n be i.i.d. copies of W . Split $\{1, \dots, n\}$ into $J \geq 2$ folds I_1, \dots, I_J with $|I_j| \rightarrow \infty$ and J fixed. For each fold j , fit an estimator $\hat{g}^{(-j)}$ using only data in $\{W_i : i \notin I_j\}$, and enforce $\hat{g}^{(-j)}(z, \hat{y}) \in [\varepsilon, 1]$ for some fixed $\varepsilon \in (0, 1)$ (e.g. by clipping). For each $i \in I_j$, set $\hat{g}_i := \hat{g}^{(-j)}$ and $C_i := C_{\hat{g}_i}(W_i)$. Define the empirical risk

$$\hat{R}_n(\theta) := \frac{1}{n} \sum_{i=1}^n \ell_\theta(C_i, X_i).$$

B.2. Main result

We will work on the following assumptions standard in semi-parametric statistics (Kang & Schafer, 2007; Wager & Athey, 2018; Angelopoulos et al., 2023).

Assumption B.1 (MAR depending only on (Z, \hat{Y})). $\mathbb{P}(A = 1 \mid X, Z, Y, \hat{Y}) = g^*(Z, \hat{Y})$ almost surely.

Assumption B.2 (Positivity). There exists $\varepsilon > 0$ such that $g^*(Z, \hat{Y}) \geq \varepsilon$ almost surely.

Assumption B.3 (Bounded log score at fixed θ). There exists $M_\theta < \infty$ such that $\max_{1 \leq k \leq K} |s_{\theta, k}(X)| \leq M_\theta$ almost surely. Equivalently, $\max_{1 \leq k \leq K} |\log p_\theta(k \mid X)| \leq M_\theta$ almost surely.

Assumption B.4 (Cross-fitted range constraint). For each fold j , the fitted $\hat{g}^{(-j)}$ satisfies $\hat{g}^{(-j)}(z, \hat{y}) \in [\varepsilon, 1]$ for all (z, \hat{y}) .

We will show consistency under either of the following alternative conditions:

- (G) Propensity consistency: $\mathbb{E}[|\hat{g}^{(-j)}(Z, \hat{Y}) - g^*(Z, \hat{Y})|] \rightarrow 0$ for each j ,
- (Y) Proxy label consistency: $\mathbb{P}(\hat{Y} \neq Y) \rightarrow 0$.

Theorem B.5 (Proxy-baseline AIPW corrector is doubly robust). *Assume B.1–B.4 and fix θ .*

1. Exact population bias identity (double robustness). For any measurable $g : \mathcal{Z} \times \{1, \dots, K\} \rightarrow [\varepsilon, 1]$,

$$\mathbb{E}[\ell_\theta(C_g(W), X)] - R(\theta) = \mathbb{E}\left[\frac{g(Z, \hat{Y}) - g^*(Z, \hat{Y})}{g(Z, \hat{Y})} (e(\hat{Y}) - f^*(X, Z, \hat{Y}))^\top s_\theta(X)\right].$$

In particular:

- If $g = g^*$ almost surely, then $\mathbb{E}[\ell_\theta(C_g(W), X)] = R(\theta)$ exactly.
- If $\hat{Y} = Y$ almost surely, then $f^*(X, Z, \hat{Y}) = e(\hat{Y})$ almost surely and hence $\mathbb{E}[\ell_\theta(C_g(W), X)] = R(\theta)$ for any g bounded away from 0.

2. Doubly robust consistency of the cross-fitted risk estimator. The cross-fitted estimator $\hat{R}_n(\theta)$ satisfies

$$\hat{R}_n(\theta) - R(\theta) \rightarrow 0 \quad \text{in probability as } n \rightarrow \infty,$$

provided either (G) holds or (Y) holds.

Proof. By definition of $s_\theta(X)$, we write

$$\ell_\theta(q, X) = q^\top s_\theta(X) \quad \text{for all } q \in \mathbb{R}^K.$$

Using the definition of $C_g(W)$ and the above, we have

$$\ell_\theta(C_g(W), X) = \ell_\theta(e(\hat{Y}), X) + \frac{A}{g(Z, \hat{Y})} (\ell_\theta(e(Y), X) - \ell_\theta(e(\hat{Y}), X)). \quad (10)$$

Let $V := (X, Z, \hat{Y})$ and define

$$\Delta := \ell_\theta(e(Y), X) - \ell_\theta(e(\hat{Y}), X).$$

Under Assumption B.1,

$$\mathbb{E}[A | V, Y] = \mathbb{E}[A | X, Z, Y, \hat{Y}] = g^*(Z, \hat{Y}),$$

which implies A is conditionally independent of Y given V . Therefore, by iterated expectations,

$$\mathbb{E}[A\Delta | V] = \mathbb{E}[\mathbb{E}[A\Delta | V, Y] | V] = \mathbb{E}[\mathbb{E}[A | V, Y]\Delta | V] = g^*(Z, \hat{Y})\mathbb{E}[\Delta | V].$$

Hence,

$$\mathbb{E}\left[\frac{A}{g(Z, \hat{Y})}\Delta \mid V\right] = \frac{g^*(Z, \hat{Y})}{g(Z, \hat{Y})}\mathbb{E}[\Delta | V]. \quad (11)$$

Since $s_\theta(X)$ is V -measurable (it depends only on X),

$$\mathbb{E}[\ell_\theta(e(Y), X) | V] = \mathbb{E}[e(Y)^\top s_\theta(X) | V] = \mathbb{E}[e(Y) | V]^\top s_\theta(X) = f^*(V)^\top s_\theta(X) = \ell_\theta(f^*(V), X).$$

Consequently,

$$R(\theta) = \mathbb{E}[\ell_\theta(e(Y), X)] = \mathbb{E}[\mathbb{E}[\ell_\theta(e(Y), X) | V]] = \mathbb{E}[\ell_\theta(f^*(V), X)]. \quad (12)$$

Take conditional expectations of the expansion in Eq. (10) given V and use Eq. (11):

$$\mathbb{E}[\ell_\theta(C_g(W), X) | V] = \ell_\theta(e(\hat{Y}), X) + \frac{g^*(Z, \hat{Y})}{g(Z, \hat{Y})}(\mathbb{E}[\ell_\theta(e(Y), X) | V] - \ell_\theta(e(\hat{Y}), X)).$$

Using Eq. (12) to substitute $\mathbb{E}[\ell_\theta(e(Y), X) | V] = \ell_\theta(f^*(V), X)$ gives

$$\begin{aligned} \mathbb{E}[\ell_\theta(C_g(W), X) | V] &= \ell_\theta(e(\hat{Y}), X) + \frac{g^*(Z, \hat{Y})}{g(Z, \hat{Y})}(\ell_\theta(f^*(V), X) - \ell_\theta(e(\hat{Y}), X)) \\ &= \ell_\theta(f^*(V), X) + \left(1 - \frac{g^*(Z, \hat{Y})}{g(Z, \hat{Y})}\right)(\ell_\theta(e(\hat{Y}), X) - \ell_\theta(f^*(V), X)). \end{aligned}$$

By linearity,

$$\ell_\theta(e(\hat{Y}), X) - \ell_\theta(f^*(V), X) = (e(\hat{Y}) - f^*(V))^\top s_\theta(X).$$

Therefore,

$$\mathbb{E}[\ell_\theta(C_g(W), X) | V] - \ell_\theta(f^*(V), X) = \frac{g(Z, \hat{Y}) - g^*(Z, \hat{Y})}{g(Z, \hat{Y})}(e(\hat{Y}) - f^*(V))^\top s_\theta(X). \quad (13)$$

Taking unconditional expectations and using $R(\theta) = \mathbb{E}[\ell_\theta(f^*(V), X)]$ yields the stated bias identity.

The first claim follows immediately: if $g = g^*$ then the multiplicative factor is 0 almost surely; if $\hat{Y} = Y$ almost surely then Y is V -measurable and hence $f^*(V) = \mathbb{E}[e(Y) | V] = e(\hat{Y})$ almost surely.

Under Assumption B.4, $g(Z, \hat{Y}) \geq \varepsilon$. Since $\|e(Y)\|_1 = 1$ and $\|e(Y) - e(\hat{Y})\|_1 \leq 2$,

$$\|C_g(W)\|_1 \leq \|e(\hat{Y})\|_1 + \frac{A}{g(Z, \hat{Y})}\|e(Y) - e(\hat{Y})\|_1 \leq 1 + \frac{2}{\varepsilon}.$$

By Assumption B.3, $\|s_\theta(X)\|_\infty \leq M_\theta$ almost surely, so

$$|\ell_\theta(C_g(W), X)| = |C_g(W)^\top s_\theta(X)| \leq \|C_g(W)\|_1 \|s_\theta(X)\|_\infty \leq \left(1 + \frac{2}{\varepsilon}\right) M_\theta. \quad (14)$$

Fix a fold j and write the fold average

$$\hat{R}_{n,j}(\theta) := \frac{1}{|I_j|} \sum_{i \in I_j} \ell_\theta(C_{\hat{g}^{(-j)}}(W_i), X_i).$$

Condition on the training data used to fit $\hat{g}^{(-j)}$ (i.e. on $\{W_i : i \notin I_j\}$). By cross-fitting, the summands for $i \in I_j$ are i.i.d. given the training data, and bounded by Eq. (14). Therefore, Chebyshev's inequality (conditional on the training data) yields

$$\hat{R}_{n,j}(\theta) - \mathbb{E}[\ell_\theta(C_{\hat{g}^{(-j)}}(W), X) \mid \{W_i : i \notin I_j\}] \rightarrow 0 \quad \text{in probability.}$$

Averaging over $j = 1, \dots, J$ and using that J is fixed gives

$$\hat{R}_n(\theta) - \bar{\mu}_n(\theta) \rightarrow 0 \quad \text{in probability,} \quad (15)$$

where

$$\bar{\mu}_n(\theta) := \sum_{j=1}^J \frac{|I_j|}{n} \mathbb{E}[\ell_\theta(C_{\hat{g}^{(-j)}}(W), X) \mid \{W_i : i \notin I_j\}].$$

Fix j . Conditional on the training data, $\hat{g}^{(-j)}$ is deterministic and belongs to $[\varepsilon, 1]$. Apply the population identity from Eq. (13) with $g = \hat{g}^{(-j)}$ and then take absolute values:

$$\begin{aligned} & \left| \mathbb{E}[\ell_\theta(C_{\hat{g}^{(-j)}}(W), X) \mid \{W_i : i \notin I_j\}] - R(\theta) \right| \\ & \leq \mathbb{E} \left[\left| \frac{\hat{g}^{(-j)}(Z, \hat{Y}) - g^*(Z, \hat{Y})}{\hat{g}^{(-j)}(Z, \hat{Y})} \right| \left| (e(\hat{Y}) - f^*(V))^\top s_\theta(X) \right| \mid \{W_i : i \notin I_j\} \right] \\ & \leq \frac{M_\theta}{\varepsilon} \mathbb{E} \left[|\hat{g}^{(-j)}(Z, \hat{Y}) - g^*(Z, \hat{Y})| \|e(\hat{Y}) - f^*(V)\|_1 \mid \{W_i : i \notin I_j\} \right], \end{aligned}$$

using $\|s_\theta(X)\|_\infty \leq M_\theta$ and $\hat{g}^{(-j)} \geq \varepsilon$. Since $\|e(\hat{Y}) - f^*(V)\|_1 \leq 2$, we further have

$$\left| \mathbb{E}[\ell_\theta(C_{\hat{g}^{(-j)}}(W), X) \mid \{W_i : i \notin I_j\}] - R(\theta) \right| \leq \frac{2M_\theta}{\varepsilon} \mathbb{E} \left[|\hat{g}^{(-j)}(Z, \hat{Y}) - g^*(Z, \hat{Y})| \mid \{W_i : i \notin I_j\} \right].$$

Thus, under condition (G) we get the conditional mean converges to $R(\theta)$ in probability.

Under condition (Y), we instead use the *exact* identity

$$\mathbb{E}[\|e(\hat{Y}) - f^*(V)\|_1] = 2\mathbb{P}(\hat{Y} \neq Y),$$

due to the following: letting $j := \hat{Y}$ and writing $f_k^*(V) = \mathbb{P}(Y = k \mid V)$,

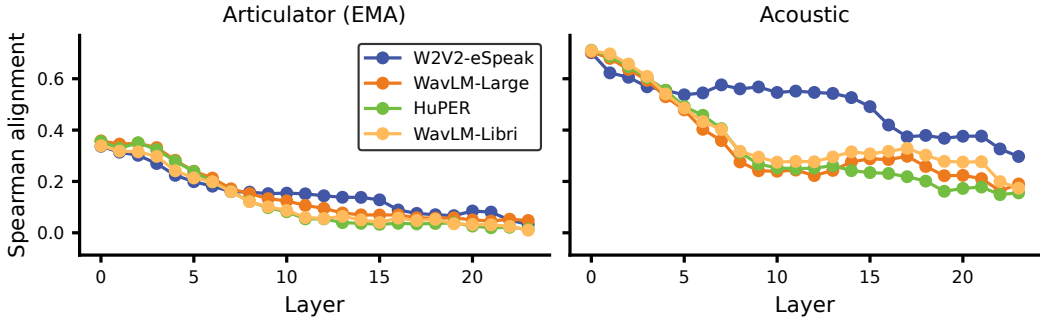
$$\begin{aligned} \|e(\hat{Y}) - f^*(V)\|_1 &= |1 - f_j^*(V)| + \sum_{k \neq j} |0 - f_k^*(V)| = (1 - f_j^*(V)) + \sum_{k \neq j} f_k^*(V) = 2(1 - f_j^*(V)) \\ &= 2(1 - \mathbb{P}(Y = \hat{Y} \mid V)). \end{aligned}$$

Taking expectations yields $2(1 - \mathbb{E}[\mathbb{P}(Y = \hat{Y} \mid V)]) = 2(1 - \mathbb{P}(Y = \hat{Y})) = 2\mathbb{P}(\hat{Y} \neq Y)$. Hence (Y) implies $\mathbb{E}[\|e(\hat{Y}) - f^*(V)\|_1] \rightarrow 0$. Returning to the bound, the same consistency statement follows due to $|\hat{g}^{(-j)} - g^*| \leq 1$ and $\hat{g}^{(-j)} \geq \varepsilon$. Combining across folds leads to $\bar{\mu}_n(\theta) - R(\theta) \rightarrow 0$ in probability under either (G) or (Y).

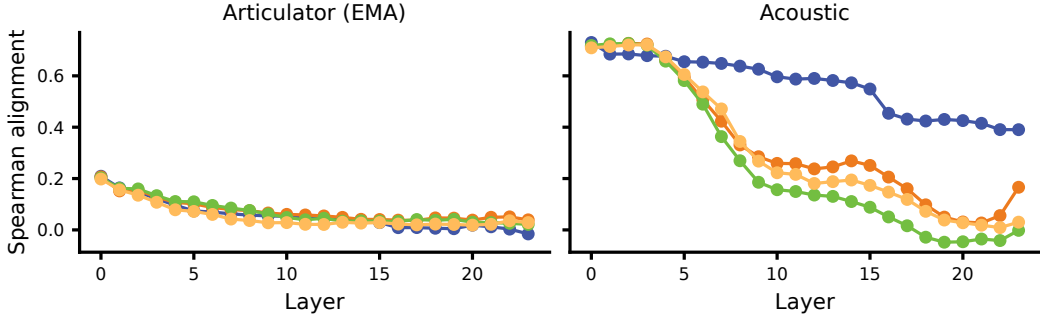
With the above step and Eq. (15), we have

$$\hat{R}_n(\theta) - R(\theta) = (\hat{R}_n(\theta) - \bar{\mu}_n(\theta)) + (\bar{\mu}_n(\theta) - R(\theta)) \rightarrow 0 \quad \text{in probability,}$$

thus establishing the consistency claim. \square



(a) **Within-phone (same phone).** Segment pairs are sampled from the same phone label. We report layer-wise Spearman correlation between embedding cosine distances and reference cosine distances (EMA vs. acoustic), after subtracting a shuffled-reference baseline.



(b) **Overall (mostly different phones).** Segment pairs are sampled uniformly from all segments (thus mainly different phone labels). Same metric as above.

Figure 8. Zero-shot alignment to acoustic and articulatory references on MOCHA-TIMIT. Articulatory (EMA) alignment is weak and not diagnostic, and raw acoustic alignment provides limited separation among models.

C. Zero-shot alignment to acoustic and articulatory references

To complement Sec. 8.1, we run a segment-level, zero-shot reference-alignment analysis on MOCHA-TIMIT¹, which provides paired audio and EMA measurements. This analysis asks whether model embeddings preserve similarity structure induced by (i) raw acoustics and (ii) articulatory trajectories.

Reference spaces. For each phone segment, we compute an **acoustic** reference vector by averaging an 80-dim log-mel spectrogram over frames. We compute an **articulatory (EMA)** reference vector by averaging the 20-dim EMA coordinates within the segment (after utterance-level de-meaning and keeping frames marked as present). We ℓ_2 -normalize reference vectors and use cosine distance.

Embedding distances and RSA. For each model and transformer layer, we mean-pool hidden states over frames inside each phone segment to obtain a segment embedding, then ℓ_2 -normalize it and compute cosine distances on sampled segment pairs. We report Spearman correlation between embedding distances and reference distances, and subtract a shuffled-reference correlation as a small random baseline (so values near zero indicate no reliable alignment).

Within-phone vs. overall pairs. We evaluate two pairing regimes: **within-phone** samples pairs of segments that share the *same* phone label (probing variability across different realizations of the same phone), while **overall** samples pairs uniformly from all segments (mostly *different* phones, probing global geometry).

Key observations. Figure 8a–8b supports two takeaways.

First, **articulatory (EMA) alignment is weak**. Across both within-phone and overall regimes, EMA alignment is modest in the earliest layers and quickly collapses toward zero in mid/late layers, with little separation between models. This indicates

¹<https://www.cstr.ed.ac.uk/research/projects/artic/mocha.html>

that, under a simple segment-mean EMA summary, embeddings do not preserve a stable articulatory similarity geometry across depth.

Second, **raw acoustic alignment is also not diagnostic for comparing models**. All models show similarly high early-layer alignment to log-mel similarity, and the curves provide limited separation among HuPER, WavLM-Raw, and WavLM-Libri (even when trends diverge later). As a result, a pure acoustic reference does not clearly reveal where HuPER’s improvements come from. This motivates our main-paper focus on a more controlled *acoustic-phonetic* reference (PanPhon distinctive-feature geometry), which is less entangled with nuisance factors and yields clearer, more interpretable cross-model differences.

D. Phonetic Feature Error Rate (PFER)

Following prior work, we use PFER (Mortensen et al., 2016), an articulatory-feature edit distance based on PanPhon distinctive features. Let $\text{feat}(p) \in \{0, 1\}^{24}$ denote the 24-dimensional binary distinctive-feature vector for phone p . For a substitution $p \rightarrow q$, the cost is the normalized Hamming distance in feature space:

$$d_{\text{sub}}(p, q) = \frac{1}{24} \|\text{feat}(p) - \text{feat}(q)\|_1. \quad (16)$$

Insertions and deletions each have unit cost. Let $D(\hat{Y}, Y)$ be the minimum-cost Levenshtein distance between the predicted phone sequence \hat{Y} and the reference sequence Y under these costs. We normalize by the reference length:

$$\text{PFER}(\hat{Y}, Y) = \frac{1}{|Y|} D(\hat{Y}, Y). \quad (17)$$

Compared to exact-match PER, PFER assigns partial credit to substitutions that differ in only a small number of distinctive features (e.g., voicing).

E. Failure cases study

We analyze failure modes on PPA to understand when (i) bottom-up phone evidence collapses, (ii) WFST-based top-down refinement hurts, and (iii) distortion-based switching makes suboptimal routing decisions. For each utterance we consider three routes available at test time: *1-best* (bottom-up), *refine* (WFST refinement conditioned on the predicted transcript), and *switch* (distortion-controlled selection between 1-best and refine). For diagnosis only, we additionally report *refine_{given}*, i.e., refinement conditioned on an external reference transcript (not available at test time).

E.1. Case selection protocol

We select representative cases using three reproducible criteria: (1) highest PFER under 1-best, (2) largest degradation from refinement ($\Delta = \text{PFER}_{\text{ref}} - \text{PFER}_{1b}$), and (3) largest *switching regret* defined as $\text{PFER}_{\text{sw}} - \min(\text{PFER}_{1b}, \text{PFER}_{\text{ref}})$. To compute the switching route in this appendix, we use a fixed threshold $\tau = 0.573$ on the distortion score (chosen to minimize mean PFER on this evaluation set). We omit utterance identifiers and audio references for privacy.

E.2. Failure taxonomy

We categorize failures into four practical types: **(A) Extreme evidence failures**, where 1-best exhibits large insertion bursts or very short phone references make the metric unstable; **(B) Wrong hypothesis conditioning**, where refine hurts but refine_{given} would help, indicating that the guiding hypothesis (predicted transcript) is incorrect; **(C) Over-constrained top-down**, where both refine and refine_{given} hurt, suggesting pronunciation coverage or LM bias issues; and **(D) Distortion/scheduler outliers**, where distortion-based routing makes noticeable mistakes (false positives/negatives) or distortion is weakly aligned with PFER for that sample.

E.3. Representative examples and aggregate summary

Table 4 lists representative examples for each failure type, and Table 3 summarizes aggregate statistics by category.

Category	<i>n</i>	Dist.	PFER _{1b}	PFER _{ref}	Δ	Regret
Extreme evidence failures	5	0.614	2.214	1.023	-1.191	0.000
Wrong hypothesis conditioning	11	0.570	0.277	0.551	0.274	0.093
Over-constrained top-down	16	0.563	0.223	0.422	0.199	0.089
Distortion/scheduler outliers	5	0.512	0.751	0.585	-0.167	0.174
Other	37	0.543	0.290	0.305	0.016	0.018

Table 3. Aggregate statistics by failure category. $\Delta = \text{PFER}_{\text{ref}} - \text{PFER}_{1b}$. Regret is computed for distortion switching with $\tau = 0.573$.

E.4. Implications

Across (B) and (C), a recurring pattern is that hard constraints can hurt unless the guiding hypothesis is reliable and the pronunciation model has sufficient coverage for weak/atypical realizations. In practice, we found the following mitigations useful: (i) hypothesis ensembling (e.g., ASR N -best) when conditioning refinement; (ii) softening constraints by tuning LM weight/word insertion penalty and expanding pronunciation variants; and (iii) sanity checks to flag extremely short references or insertion bursts before interpreting PFER.

E.5. Concrete error snippets

Red marks phones/words that are not aligned to the reference (substitutions/insertions). Deleted reference phones are shown with ~~on~~ on the GT line. A red underscore indicates an empty counterpart in the alignment.

Case A1. Reference text: Twice each day he plays skillfully and with zest upon a small organ

Predicted hypothesis (for refinement): twice a day he **place** **skilly** and with **zeppa** **pounce** **mogin**

Distortion: 0.597. **PFER**_{1b}=3.638, **PFER**_{ref}=2.350, **PFER**_{given}=2.258.

Extreme evidence failure with a large insertion burst; both routes struggle.

GT: ~~-~~ EH ~~-~~ N ~~-~~ HH IY S ~~-~~ P

1-best: **+K** **+IH** EH **+L** **+L** **+IY** **+IH** N **+D** **+W** **+IH** **+TH** **+Z** EH P S **+AH** P

refine: ~~-~~ ~~-~~ ~~-~~ N D ~~-~~ ~~-~~ ~~-~~

Case A2. Reference text: yet he still thinks as swiftly as ever

Predicted hypothesis (for refinement): citizen

Distortion: 0.643. **PFER**_{1b}=3.225, **PFER**_{ref}=0.250, **PFER**_{given}=1.800.

Very short phone reference; refinement can sharply reduce insertion-driven PFER but may be unstable.

GT: Y EH T HH IY S T IH L TH IH NG K S AE Z S W IH F T L IY AE Z EH V ER

1-best: **+S** **+IH** **+T** **+IH** **+Z** **+AH** **+N** **+CH** **+AH** **+N** **+T** **+S** **+AH** **+N** **+CH** **+AH** **+N** **+T**

refine: Y EH T HH IY S T IH L TH IH NG K S AE Z S W IH F T L IY AE Z EH V ER

Case B1. Reference text: When he speaks

Predicted hypothesis (for refinement): he **spake**

Distortion: 0.496. **PFER**_{1b}=0.163, **PFER**_{ref}=0.483, **PFER**_{given}=0.208.

Wrong-hypothesis conditioning: refinement is guided by an incorrect word form (“spake”), distorting constraints.

GT: HH EH N HH IY S P IY K S

1-best: HH IY **Z** **S** P IY K S

refine: HH IY **S** P **EY** K

Case B2. Reference text: Well he is nearly ninety three years old

Predicted hypothesis (for refinement): well **nigh** **thistle**

Distortion: 0.649. **PFER**_{1b}=0.357, **PFER**_{ref}=0.663, **PFER**_{given}=0.312.

Wrong-hypothesis conditioning: hypothesis is far from the reference, so refinement degrades phone accuracy.

HuPER: A Human-Inspired Framework for Phonetic Perception

Case	Ref text (abbr.)	Dist.	PFER _{1b}	PFER _{ref}	PFER _{given}	PFER _{sw}	Diagnosis
A. Extreme evidence failures							
A1	Twice each day he plays skillfully and with zest ...	0.597	3.638	2.350	2.258	2.350	1-best insertion burst; refine stabilizes.
A2	yet he still thinks as swiftly as ever	0.643	3.225	0.250	1.800	0.250	Short phone ref; insertion dominates.
A3	Grandfather likes to be modern in his language	0.656	1.783	1.022	0.395	1.022	1-best insertion burst; refine stabilizes.
A4	giving those who observe him a pronounced feeling of ...	0.593	1.359	0.915	0.859	0.915	Both routes fail; weak evidence.
B. Wrong hypothesis conditioning							
B1	Well he is nearly ninety three years old	0.649	0.357	0.663	0.312	0.663	Hypothesis mismatch: ref-conditioned refine hurts; Given ref helps.
B2	When he speaks	0.496	0.163	0.483	0.208	0.163	Hypothesis mismatch: ref-conditioned refine hurts; Given ref helps.
B3	He dresses himself in an old black frock coat	0.568	0.243	0.635	0.364	0.243	Hypothesis mismatch: ref-conditioned refine hurts; Given ref helps.
B4	He dresses himself in an old black frock coat	0.605	0.430	0.765	0.500	0.765	Hypothesis mismatch: ref-conditioned refine hurts; Given ref helps.
C. Over-constrained top-down							
C1	but he always answers Banana oil	0.585	0.150	0.556	0.679	0.556	Over-constraint: refine hurts even with Given ref.
C2	but he always answers Banana oil	0.617	0.361	0.703	0.696	0.703	Over-constraint: refine hurts even with Given ref.
C3	A long beard clangs to his chin	0.560	0.242	0.554	0.554	0.242	Over-constraint: refine hurts even with Given ref.
C4	Yet he still thinks as swiftly as ever	0.643	0.286	0.591	0.535	0.591	Over-constraint: refine hurts even with Given ref.
D. Distortion/scheduler outliers							
D1	usually several buttons are missing	0.589	0.240	0.619	0.619	0.619	Scheduler FP: high distortion but refine hurts.
D2	but he always answers Banana oil	0.566	0.657	0.361	0.404	0.657	Scheduler FN: low distortion but refine would help.
D3	giving those who observe him a pronounced feeling of ...	0.553	0.951	0.656	0.719	0.951	Scheduler FN: low distortion but refine would help.
D4	he slowly takes a short walk in the open ...	0.519	0.663	0.422	0.422	0.663	Scheduler FN: low distortion but refine would help.

Table 4. Representative failure cases on PPA. Dist. is the distortion score. PFER_{1b} is HuPER 1-best, PFER_{ref} is refinement conditioned on the predicted transcript, PFER_{given} is refinement conditioned on an external reference transcript, and PFER_{sw} is distortion-controlled switching with $\tau = 0.573$.

GT: W EH L HH IY IH Z N IH R L IY N AY N T IY TH R IY Y IH R Z OW L D
 1-best: W EH L HH IY IH Z N IH R L IY N AY N S IY TH R IY S AH L D
 refine: W EH L N AY TH AH S AH L

Case C1. Reference text: but he always answers Banana oil

Predicted hypothesis (for refinement): **business boil**

Distortion: 0.585. **PFER_{1b}**=0.150, **PFER_{ref}**=0.556, **PFER_{given}**=0.679.

Over-constrained top-down: even with the correct transcript, refinement hurts (pronunciation/LM bias).

GT: B AH T HH IY AO L W EY Z AE N S ER Z B AH N AE N AH OY L
 1-best: B AH T HH IY AO L W EY Z AE N S ER Z B AH N AE N AH OY L
 refine: B IH Z N AH S B OY L

Case C2. Reference text: A long beard clangs to his chin

Predicted hypothesis (for refinement): **henri kisses chin**

Distortion: 0.560. **PFER_{1b}**=0.242, **PFER_{ref}**=0.554, **PFER_{given}**=0.554.

Over-constrained top-down on a short phrase; refinement introduces consistent substitutions.

GT: AH L AO NG B IH R D K L IH NG Z T UW HH IH Z CH IH N
 1-best: AH **L** AO NG B IH R D K L IH NG Z T UW HH IH Z CH IH N
 refine: HH EH N R IY K IH S AH Z CH IH N

Case D1. Reference text: but he always answers Banana oil

Predicted hypothesis (for refinement): but he **has** he **was** answers banana

Distortion: 0.566. **PFER**_{1b}=0.657, **PFER**_{ref}=0.361.

Scheduler false negative at $\tau = 0.573$: distortion is below threshold so switching keeps 1-best, but refinement would help.

GT: B AH T HH IY AO L W EY Z AE N S ER Z B AH N AE N AH OY L
 1-best: S P B AH **DX** HH IY HH AE **Z** HH IY **W** AA Z AE N S ER Z B AH N AE N AH
 refine: B AH T HH IY **HH** AE Z HH IY W AA Z AE N S ER Z B AH N AE N AH OY L

Case D2. Reference text: giving those who observe him a pronounced feeling of the utmost respect

Predicted hypothesis (for refinement): giving those who observe him **announced filling** of the **upmost** respect

Distortion: 0.553. **PFER**_{1b}=0.951, **PFER**_{ref}=0.656.

Scheduler false negative at $\tau = 0.573$: switching keeps 1-best but refinement reduces PFER under weak evidence.

GT: G IH V IH NG DH OW Z HH UW AH B Z ER V HH IH M EY P R AH N AW N S T F IY L
 IH NG AH V DH AH AH T ER M OW S T R IH S P EH K T
 1-best: G IH V IH NG **N** DH OW Z HH UW AH B **Z** ER V HH IH M **AH N UH** N S T F IY L IH
 NG AH V **DH** AH
 refine: G IH V IH NG DH OW Z HH UW AH B Z ER V HH IH M EY P R AH N AW N S T F IY L
 IH NG AH V DH AH

F. Analysis details for understanding HuPER-Recognizer gains

F.1. Centroid RSA: setup and implementation

Goal. We quantify whether an encoder’s phone representations are organized by broad acoustic–phonetic similarity, using PanPhon distinctive-feature distances as a controlled proxy (Mortensen et al., 2016).

Data. We run the analysis on TIMIT, which provides time-stamped phone segments. Each segment is associated with a phone label.

Phone representations. At each transformer layer ℓ , we extract hidden states and mean-pool within each phone segment to obtain a segment embedding. We then average segment embeddings of the same phone to form a phone centroid $\mathbf{c}^{(\ell)}(p)$.

Distances and RSA score. We compute pairwise cosine distances between phone centroids to form an embedding-distance matrix $D_{\text{emb}}^{(\ell)}$. We also compute a PanPhon feature-distance matrix D_{pan} over the same phone set. The layer-wise RSA score is the Spearman correlation between vectorized upper triangles of $D_{\text{emb}}^{(\ell)}$ and D_{pan} .

Label-set normalization. To compare models with different label spaces, we map each model’s predicted/annotated phone labels into HuPER’s compact inventory before computing both centroids and PanPhon distances. Provide the mapping rules/table here (or reference your script/config):

Models compared. We include (i) *W2V2-eSpeak* (multilingual phone recognition baseline), (ii) *WavLM-Raw* (pretrained WavLM-Large), (iii) *WavLM-Libri* (English-only fine-tuning on LibriSpeech with G2P labels), and (iv) HuPER-Recognizer.

Reproducibility notes. Report any filtering (e.g., minimum segment duration), phone-frequency thresholds, and how you handle silences/closures if applicable.

F.2. Emission diagnostic: construction, scoring, and text inputs

We use a controlled diagnostic to test whether CTC emissions prefer the *canonical* (G2P) phone sequence or the *realized* phone sequence supported by the acoustics.

Diagnostic set. We focus on three cases where canonical restoration is tempting in casual English speech: **glottalization**, **flaps**, and **stops in consonant clusters**. For each synthesized utterance waveform x , we create a matched contrast $(x, y_{\text{can}}, y_{\text{real}})$: y_{can} is the canonical G2P phone sequence, and y_{real} is a realized phone sequence verified by listening.

CTC evidence. Given a CTC recognizer, we compute the marginal log-likelihood $\log P(y | x)$ via the forward algorithm in log-space. To compare sequences of different lengths, we use a per-phone normalized preference score:

$$\Delta_{\text{norm}}(x) = \frac{\log P(y_{\text{can}} | x)}{|y_{\text{can}}|} - \frac{\log P(y_{\text{real}} | x)}{|y_{\text{real}}|}. \quad (18)$$

$\Delta_{\text{norm}} > 0$ indicates canonical-restoring emissions, while $\Delta_{\text{norm}} < 0$ indicates acoustic-faithful emissions favoring the realized sequence.

Reporting. In the main paper, we plot per-utterance scores for HuPER vs. the XLSR baseline (Fig. 7). We also report a compact category-wise summary:

Category	HuPER-Recognizer (ours)		XLSR baseline		Paired diff (XLSR – Ours)	
	median Δ_{norm}	$\Pr(\Delta_{\text{norm}} > 0)$	median Δ_{norm}	$\Pr(\Delta_{\text{norm}} > 0)$	median Δ_{norm}	$\Pr(> 0)$
Glottalization	−1.018	0.00	+0.889	0.70	+1.535	1.00
Flaps	−0.768	0.00	−0.459	0.30	+0.630	0.90
Stops in clusters	−0.424	0.20	+0.413	0.90	+0.886	0.80

Table 5. Emission-level diagnostic using Δ_{norm} . $\Delta_{\text{norm}} > 0$ indicates that emissions prefer the canonical phone sequence over the realized sequence. The paired-difference columns compare the two models on the same utterances; positive values mean the XLSR baseline is more canonical-restoring than HuPER-Recognizer.

Text inputs (plain text only). This appendix also records the exact text inputs used to synthesize the diagnostic waveforms referenced in Sec. 8.2. All inputs are plain text (no style tags or special TTS instructions). We generate short, TTS-friendly phrases using a single prompt template (run once per category):

Generate 10 short English phrases (2–4 words) that are likely to be pronounced in casual speech with the following phenomenon: {PHENOMENON}.
 Constraints: common words, no proper nouns, keep it short and natural for TTS.
 Return only the 10 phrases, one per line.

The resulting phrases (10 per category) are listed in Table 6. After audio generation, each item is manually checked and paired with $(y_{\text{can}}, y_{\text{real}})$ for the emission test.

Glottalization	Flaps	Stops in consonant clusters
a button	a better idea	last Sunday
my kitten	a little later	next day
that mountain	water bottle	just say
in Britain	get it	best friend
a little bit	put it away	first time
not now	what a day	most people
can't go	write it down	west side
get back	I need it	old man
sit down	go to bed	hand bag
at night	it is ready	asked to

Table 6. Text inputs used to synthesize the emission diagnostic set in Sec. 8.2 (plain text only; 10 per category).

Table 7. Evaluation datasets for phone recognition.

Dataset	Description
Buckeye (Pitt et al., 2005)	Natural English conversational speech with human phonetic annotation.
DRC-SE (DoReCo South-England) (Paschen et al., 2020)	English dialectal-variation subset from DoReCo (South England).
L2-ARCTIC-Perceived (Zhao et al., 2018)	L2 English speech corpus with human-verified / annotated pronunciations.
EpaDB (Vidal et al., 2019)	L2 English (Spanish-accented) speech with detailed phonetic annotations (e.g., mispronunciations).
Speech Ocean762 (Zhang et al., 2021)	Large-scale L2 English corpus with human annotations / verification.
VoxAngeles (Chodroff et al., 2024)	Multilingual word recordings; evaluate on languages such as Chamorro, Degema, Lakota, Pampanga, Iloko, etc.

 Table 8: **Zero-shot multilingual phone recognition on VoxAngeles.** Per-language PFER is reported (lower is better). Entries of 1.00 mean the model lacks support for the corresponding language/inventory. Red highlights languages where HuPER attains the best (lowest) PFER across all baselines.

language	Allosaura	Wav2Vec2Phoneme	MultIPA	ZIPA	Allophant	HuPER
abk	0.61	0.40	0.32	0.44	1.00	0.35
ace	0.24	0.18	0.15	0.15	1.00	0.29
ady	0.36	0.32	0.35	0.32	1.00	0.30
aeb	0.32	0.17	0.17	0.25	1.00	0.17
afn	0.20	0.10	0.11	0.21	1.00	0.14
afr	0.23	0.11	0.14	0.16	1.00	0.10
agx	0.25	0.20	0.17	0.16	1.00	0.30
ajp	0.38	0.12	0.13	0.21	1.00	0.12
aka	0.20	0.10	0.13	0.18	1.00	0.14
apc	0.25	0.14	0.13	0.14	1.00	0.18
ape	0.34	0.17	0.14	0.15	1.00	0.19
apw	0.30	0.19	0.18	0.21	1.00	0.10
asm	0.21	0.10	0.09	0.18	1.00	0.20
azb	0.25	0.15	0.12	0.18	1.00	0.20
bam	0.27	0.22	0.23	0.32	1.00	0.28

Continued on next page

Table 8: **Zero-shot multilingual phone recognition on VoxAngloes.** Per-language PFER is reported (lower is better). Entries of 1.00 mean the model lacks support for the corresponding language/inventory. Red highlights languages where HuPER attains the best (lowest) PFER across all baselines. (Continued)

bem	0.14	0.08	0.05	0.07	1.00	0.08
ben	0.32	0.27	0.24	0.28	0.18	0.40
bfd	0.35	0.17	0.17	0.21	1.00	0.27
bfq	0.21	0.20	0.15	0.31	1.00	0.20
bhk	0.28	0.14	0.12	0.13	1.00	0.14
bin	0.19	0.08	0.10	0.17	1.00	0.12
brv	0.36	0.28	0.29	0.26	1.00	0.27
bsq	0.33	0.20	0.22	0.30	1.00	0.05
bwr	0.24	0.10	0.15	0.14	1.00	0.10
cbv	0.30	0.25	0.25	0.25	1.00	0.47
ces	0.21	0.10	0.08	0.13	0.09	0.08
cha	0.16	0.05	0.06	0.15	1.00	0.06
cji	0.40	0.30	0.21	0.47	1.00	0.32
col	0.38	0.27	0.30	0.31	1.00	0.25
cpn	0.26	0.17	0.19	0.35	1.00	0.17
dag	0.30	0.17	0.14	0.34	1.00	0.16
dan	0.24	0.16	0.19	0.23	0.24	0.18
deg	0.13	0.07	0.07	0.06	1.00	0.07
dyo	0.17	0.07	0.12	0.16	1.00	0.13
efi	0.22	0.09	0.10	0.20	1.00	0.20
ell	0.18	0.07	0.05	0.08	0.13	0.13
ema	0.26	0.10	0.21	0.17	1.00	0.24
eus	0.40	0.07	0.08	0.09	0.05	0.08
ewe	0.36	0.14	0.18	0.33	1.00	0.22
ffm	0.22	0.12	0.12	0.16	1.00	0.17
fin	0.21	0.13	0.11	0.15	0.14	0.12
fub	0.19	0.06	0.09	0.16	1.00	0.16
gaa	0.25	0.17	0.20	0.23	1.00	0.26
gla	0.32	0.14	0.16	0.30	1.00	0.18
guj	0.18	0.13	0.14	0.16	1.00	0.18
gwx	0.54	0.21	0.24	0.24	1.00	0.16
hak	0.30	0.17	0.17	0.23	1.00	0.18
hau	0.12	0.11	0.07	0.15	1.00	0.16
haw	0.21	0.12	0.14	0.14	1.00	0.15
heb	0.26	0.11	0.16	0.15	1.00	0.21
hil	0.21	0.11	0.12	0.15	1.00	0.12

Continued on next page

Table 8: **Zero-shot multilingual phone recognition on VoxAngeles.** Per-language PFER is reported (lower is better). Entries of 1.00 mean the model lacks support for the corresponding language/inventory. Red highlights languages where HuPER attains the best (lowest) PFER across all baselines. (Continued)

hin	0.27	0.12	0.07	0.17	0.09	0.15
hni	0.37	0.19	0.22	0.27	1.00	0.57
hrv	0.21	0.09	0.11	0.13	1.00	0.16
hun	0.30	0.15	0.15	0.26	0.16	0.10
hye	0.26	0.10	0.11	0.13	1.00	0.17
ibb	0.20	0.12	0.15	0.22	1.00	0.23
ibo	0.30	0.15	0.14	0.22	1.00	0.30
idu	0.23	0.13	0.12	0.16	1.00	0.19
ilo	0.17	0.10	0.09	0.13	1.00	0.12
isl	0.25	0.15	0.12	0.16	1.00	0.15
its	0.64	0.11	0.18	0.29	1.00	0.20
kan	0.18	0.10	0.07	0.12	1.00	0.07
kea	0.31	0.24	0.20	0.25	1.00	0.13
khm	0.27	0.22	0.21	0.24	1.00	0.15
klu	0.37	0.17	0.21	0.28	1.00	0.22
knn	0.20	0.13	0.11	0.25	1.00	0.20
kri	0.15	0.08	0.09	0.10	1.00	0.38
kub	0.17	0.09	0.10	0.16	1.00	0.15
kye	0.25	0.20	0.18	0.28	1.00	0.29
lad	0.25	0.15	0.13	0.12	1.00	0.16
lar	0.48	0.14	0.18	0.30	1.00	0.11
lav	0.35	0.20	0.19	0.22	1.00	0.22
led	0.42	0.23	0.15	0.21	1.00	0.25
lgq	0.25	0.11	0.16	0.41	1.00	0.23
lit	0.26	0.14	0.15	0.18	0.14	0.12
lkt	0.26	0.18	0.17	0.17	1.00	0.21
lug	0.16	0.10	0.15	0.17	1.00	0.16
mak	0.29	0.17	0.19	0.18	1.00	0.25
mal	0.37	0.19	0.18	0.22	1.00	0.46
mlt	0.27	0.13	0.09	0.17	0.19	0.16
mya	0.28	0.24	0.25	0.25	1.00	0.16
njm	0.26	0.17	0.09	0.38	1.00	0.21
nld	0.20	0.13	0.13	0.14	0.20	0.13
ozm	0.22	0.14	0.16	0.18	1.00	0.19
pam	0.24	0.16	0.19	0.18	1.00	0.08
pes	0.23	0.14	0.15	0.17	1.00	0.19

Continued on next page

Table 8: **Zero-shot multilingual phone recognition on VoxAngeles.** Per-language PFER is reported (lower is better). Entries of 1.00 mean the model lacks support for the corresponding language/inventory. Red highlights languages where HuPER attains the best (lowest) PFER across all baselines. (Continued)

prs	0.27	0.16	0.17	0.20	0.99	0.17
run	0.27	0.09	0.13	0.11	1.00	0.21
sbc	0.32	0.22	0.12	0.18	1.00	0.18
tsw	0.30	0.10	0.11	0.21	1.00	0.14
tzm	0.33	0.16	0.15	0.21	1.00	0.14
wuu	0.45	0.36	0.33	0.31	1.00	0.22
yue	0.29	0.14	0.15	0.21	1.00	0.16
Avg.	0.28	0.15	0.15	0.21	0.90	0.19

Table 9. Baseline model checkpoints

Model	Checkpoint
Allosaurus	https://github.com/xinjli/allosaurus
Allophant	https://github.com/kgnlp/allophant
W2V2-eSpeak	https://huggingface.co/facebook/wav2vec2-xlsr-53-espeak-cv-ft
MultIPA	https://huggingface.co/ctaguchi/wav2vec2-large-xlsr-japlmtthufileta-ipa1000-ns
ZIPA	https://github.com/lingjzhu/zipa
POWSM	https://huggingface.co/espnet/powsm
W2V2-en	https://huggingface.co/Bluecast/wav2vec2-Phoneme